2012-07-25

The Biomechanical Implications of an Intrinsic Decompressive Pre-Load on a Posterior Dynamic Stabilization System

Jeffrey Ellis Harris
Brigham Young University - Provo

The Biomechanical Implications of an Intrinsic Decompressive Pre-Load

on a Posterior Dynamic Stabilization System

Jeffrey E. Harris

A thesis submitted to the faculty of
Brigham Young University
in partial fulfillment of the requirements for the degree of

Master of Science

Anton E. Bowden, Chair
Steven K. Charles
Larry L. Howell

Department of Mechanical Engineering

Brigham Young University

December 2012

ABSTRACT

The Biomechanical Implications of an Intrinsic Decompressive Pre-load
on a Posterior Dynamic Stabilization System

Jeffrey E. Harris
Department of Mechanical Engineering, BYU
Master of Science

The purpose of this research was to investigate the influence of applying an intrinsic decompressive pre-load to a particular dynamic stabilization device on the biomechanical response of the lumbar spine. The FlexSPAR, which supports this ability, was used as a test case. A finite element model of a full lumbar spine was developed and validated against experimental data, and tested in the primary modes of spinal motion. The model was used to compare five lumbar spine test cases: healthy, degenerate, implanted with a pre-loaded device, implanted with a device without a pre-load, and implanted with rigid fixators.

Results indicated that a pre-loaded FlexSPAR led to improved disc height restoration and segmental biomechanics. Results also showed that a pre-loaded FlexSPAR led to less change in bone remodeling stimulus in comparison to the device without a pre-load and rigid fixators. This work shows that there is a potential to improve the performance of posterior dynamic stabilization devices by incorporating a pre-load in the device.

ACKNOWLEDGEMENTS

TABLE OF CONTENTS

LIST OF TABLES

LIST OF FIGURES

1 INTRODUCTION

1.1 Research Objectives

The objective of this research was to identify the effects of a particular posterior dynamic stabilization system, the FlexSPAR™, on the lumbar spine. Specifically, this work evaluated the influence of an intrinsic decompressive pre-load applied to the FlexSPAR on the biomechanical response of the lumbar spine. This was accomplished by developing a nonlinear finite element model of the lumbar spine. The outcomes of the research defined how the device affected disc height restoration, range of motion (ROM), bone remodeling, intradiscal pressures, load sharing, and facet contact loads.

1.2 Problem Statement

Lower back pain is a major health problem and a common condition that occurs in most individuals during some point in their life [1]. Degeneration of the intervertebral disc (IVD) is thought to be a major contributor to lower back pain and over 90% of surgical spine procedures are performed due to the consequences of IVD degeneration [2]. Disc degeneration adversely affects the biomechanics of each motion segment in the spine. The IVD is an avascular tissue that receives its nutrients through diffusion and bulk fluid flow [2]. If the diffusion process is disturbed, nutrition content drops and disc degeneration may begin.

There are many different treatment options for lower back pain (LBP) [3]. Spinal fusion has been a common method for treating spinal instability and various causes of chronic LBP over the past fifty years. Spinal fusion consists of removing the IVD and using implanted medical devices, including fusion cages and/or fusion rods to restrict motion across one or more spinal segments. By restricting segmental motion, bone growth across the segment is encouraged and mechanical triggering of pain sensing nerves (nociceptors) due to abnormal spinal motion is hopefully reduced. The long term effects of spinal fusion have often been considered to be less important than relieving the patient's current pain. However, in recent years concerns over the long term effects of spinal fusion have increased [4-6].

Spinal fusion leads to increased mechanical loading on the adjacent vertebrae. One of the consequences of spinal fusion is adjacent segment degeneration (ASD), which is the development of degenerative conditions in the neighboring vertebra [5-8]. Biomechanical studies have shown that spinal fusion increases intervertebral motion, intradiscal pressures, and facet joint stresses in the adjacent segments, which may contribute to ASD [9].

Some alternatives to spinal fusion include implanting posterior dynamic stabilization devices or total disc replacement. These types of spinal devices are increasingly being used as an alternative to fusion devices [10]. Dynamic stabilization devices act as an internal brace that allows the spine to move, but restrict motion extremes that are more likely to mechanically trigger nociceptors [11]. Like spinal fusions, dynamic stabilization devices can be inserted anteriorly or posteriorly. Many use a pedicle screw system to keep installed hardware in place. After spinal fusion, the majority of the dynamic loads exerted on the spine are withstood by the healed bone. However, in a dynamic stabilization system the pedicle screws must withstand

much of the load, which is cyclic and has been estimated at roughly three million to five million cycles per year. The nature of cyclic loading can lead to screw loosening and fatigue [10].

Pedicle-screw based motion preservation devices are intended for patients with chronic LBP who have early stage disc degeneration. Dynamic stabilization devices are intended to reduce loading on a compressed disc, and allow post-operative range of motion (ROM) to match healthy intersegmental motion [12]. This will assist in spinal stability without transferring additional stress to adjacent segments [13]. One hypothesis is that the distracted disc will be able to repair itself by allowing nutrients to re-enter the disc [11].

The FlexSPAR is a posterior dynamic stabilization device that can be inserted in the lumbar spine to provide stability. Unlike spinal fusions that restrict segmental motion, the FlexSPAR intends to allow the lumbar spine to retain its physiological biomechanics. The clinical effectiveness of dynamic stabilization devices can be determined through long term observations, or by using computational methods. In general, long term studies of PDS devices are lacking. Studying the biomechanics of the lumbar spine implanted with a FlexSPAR *in vivo* is difficult. It is therefore advantageous to use finite element modeling to understand the *in vivo* effects of the FlexSPAR in the lumbar spine. Using a finite element model is advantageous because it allows for a direct comparison between rigid fixation systems, highlighting areas where the FlexSPAR would be advantageous.

1.3   Chapter Summary

Chapter two includes a literature review of spinal anatomy, disc degeneration, adjacent segment degeneration, and current PDS devices.

Chapter three includes a review of finite element modeling techniques commonly used to model the spine. This chapter also includes the methods that were used to develop the model used in this work.

Chapter four consists of a technical paper currently being submitted for publication. The methods section of this chapter provides additional insight into the development of the model. The results and discussion section focus on the hypothesis that pre-loading a dynamic stabilization device would increase disc height restoration and improve segmental biomechanics.

Chapter five summarizes the contributions of this work and briefly suggests directions for future work.

2   BACKGROUND

This chapter reviews the anatomy of a functional spinal unit (FSU), studies on adjacent segment degeneration (ASD), current devices used to treat ASD, current finite element modeling techniques in the lumbar spine, and the FlexSPAR.

2.1   Spinal Anatomy

The human spinal column is responsible for providing support and stability while protecting the spinal cord inside the spinal canal. The lumbar spine consists of the five largest vertebrae which are responsible for the most load bearing, and where LBP is felt. Each vertebra consists of the vertebral body, pedicles, lamina, and processes. The vertebral body is responsible for carrying compressive loads. The posterior side of the vertebral body along with the pedicles and lamina make up the spinal canal, which provides protection for the spinal cord.

The IVD is an avascular, cartilaginous joint composed of the annulus fibrosus (AF), nucleus pulposus (NP), and the end plate. The AF is made of strong fibers (mostly type I collagen) that make up the outer circumference of the IVD. The AF consists of 15-25 concentric lamina that criss-cross each other at angles of approximately 30 degrees [14]. This layup allows the disc to accommodate shear and torsional forces. The collagen of the AF merges into the cartilage of the vertebral endplate and the NP.

The NP is the central portion of the disc. It is a loose collagen fibril network contained within a gelatinous matrix primarily made of type II collagen. Due to the incompressibility of the NP, compression loads are transmitted through the disc and into the vertebral body. Part of the function of the NP is to transmit vertical loads in compression, and radially direct tensile loads to the annulus fibrosus. Only the periphery of the nucleus pulposus is vascularized. The rest of the disc receives its nutrients through diffusion from the periphery of the annulus fibrosus and the vertebral endplate.

The vertebral endplates consist of thin layers of hyaline cartilage which cover the superior and inferior surfaces of the vertebral bodies. The endplates are approximately 1 millimeter thick and allow nutrient transport in and out of the disc through passive diffusion.

Lumbar spine biomechanics are commonly described using an FSU (Figure 2-1), which is the smallest physiologic motion unit of the spine. An FSU consists of an IVD sandwiched between the superior and inferior vertebrae, two facet joints, and the surrounding ligaments. The orientation of the facets in the lumbar spine allow for a primary motion of flexion-extension, although lateral bending and axial rotation occur as well.
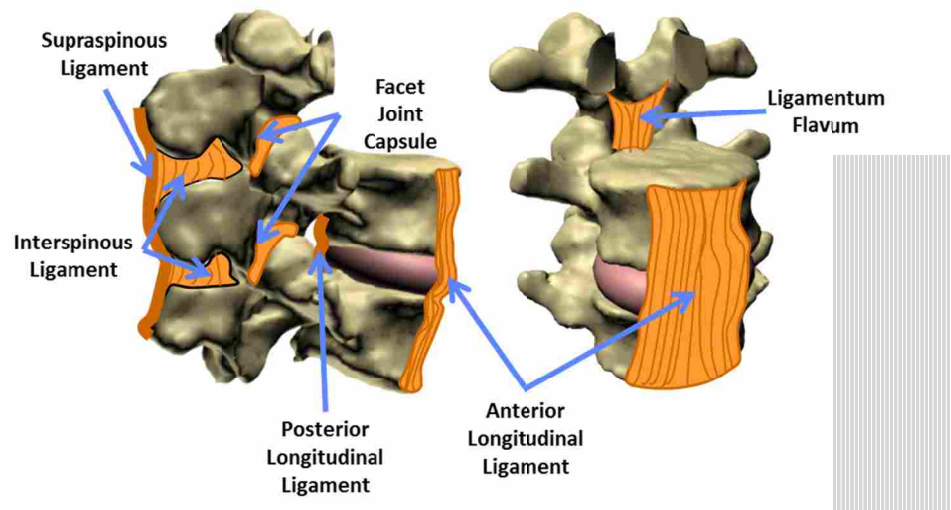
Figure 2-1: The functional spinal unit (FSU)

There are six major ligaments shown in Figure 2-1 that help provide spinal stability and connect the vertebral bodies. The anterior longitudinal ligament (ALL) and posterior longitudinal ligament (PLL) extend along the anterior and posterior surfaces vertebral column and prevent excessive flexion and extension. The ligamentum flavum (LF) extends along the posterior wall of the spinal canal. The interspinous ligament (ISL) and supraspinous ligament (SSL) insert into each other and connect between and posterior to the spinous processes, and prevent excessive flexion. The capsular ligament (CL) attaches to the edges of the articular processes and creates the facet joint capsule.

2.2   Disc Degeneration

Chronic LBP is usually the result of normal everyday living activities. The degeneration of the IVD causes the spine to gradually lose stability. Degenerative changes of the IVD can occur in the NP and AF individually, beginning with dehydration of the nucleus pulposus and hardening of the annulus fibrosus. This can lead to disc height reduction and posterior-lateral bulging of the IVD. The degeneration of the IVD can alter the physiologic pattern of motion and cause spinal instability and pain.

Disc degeneration is believed to start in the NP, where degeneration begins with a decrease in proteoglycan concentration, and a gradual change of the collagen tissue to a more fibrous tissue [15]. These changes dehydrate the IVD, which leads to an inability of the NP to transmit weight and exert pressure radially on the annulus fibrosus [16].

In the degenerate AF, the fiber patterns become disorganized, which changes the elastic response of the material [17]. The stress-strain curve of a healthy AF is highly nonlinear as shown by the toe region of the curve. In the degenerate AF, the toe region has been found to

double in tensile tests [18, 19]. As the disc degenerates, the AF begins to develop tears and fissures, which allows the nucleus pulposus to herniate. The most common disc herniation occurs posterolaterally [20].

2.3   Adjacent Segment Degeneration

Spinal fusion alters the biomechanics of the spine and can lead to increased stresses of the non-fused adjacent segments. This overloading can lead to adjacent degeneration resulting in recurring pain accompanied by neurologic symptoms. Some of the results of ASD are disc space narrowing, osteophyte formation, spinal stenosis, or disc bulging [21]. The biomechanical changes at the adjacent levels, such as an increase in ROM and increases in facet joint stresses, can lead to further degeneration. The problems fixed by fusing one segment are simply transferred to the adjacent segments, and the whole issue of LBP begins anew.

Lee et al. found that the range of motion is increased at segments adjacent to a lumbosacral fusion [22]. Weinhoffer et al. observed in simulated spinal fusions that intradiscal pressures at the levels adjacent to fusion increased, and that the intradiscal pressures continued to increase with the number of levels fused [9]. Kim et al. reported that ASD is a clinical problem in up to 20% of patients who have spinal fusion, with ASD increasing with the number of fused segments [23]. Due to the factors dynamic stabilization has received increased attention as an alternative to spinal fusion [11].

2.4   Posterior Dynamic Stabilization Systems

Dynamic stabilization is meant to restore normal segmental kinematics to the spine. This includes restoring ROM, but also a healthy quality of motion represented by the location and orientation of the instantaneous helical axes of rotation [24]. It is hypothesized that a posterior

dynamic stabilization device will prevent adjacent segment degeneration by relieving some of the load on adjacent levels when compared to fusion [25]. Since a degenerated disc does not regenerate on its own, distracting the compressed disc may create an environment that allows the disc to rehydrate and repair itself [26].

Several dynamic stabilization systems are currently used to stabilize the spine [10, 11, 27, 28]. There are shortcomings associated with each of these devices, some of which are briefly discussed in this thesis [11]. The Graf ligament was one of the first stabilization devices, and consists of bilateral pedicles screws inserted superior and inferior to the affected segment. Polypropylene bands attach to the pedicle screws which act as ligaments. The bands are tightened during extension, which will limit excessive flexion. Graf proposed that instability would be fixed if abnormal rotatory movement was stopped [28]. Facet extension due to the Graf ligament offloads the anterior annulus fibrosus, but transfers loads to the posterior annulus fibrosus, which may result in pain being felt in the disc [29, 30]. Although the bands limit excessive flexion they do nothing to limit hyper-extension. The Graf ligament becomes lax during extension and does not unload the disc during extension [11]. Hadlow reported that revision rates with individuals who received the Graf ligament is higher than those who received posterolateral fusion [27].

The Dynesys is a semi-rigid rod system similar to the Graf ligament where pedicle screws are implanted above and below the affected segment. The pedicle screws are connected with a polyethylene terephthalate (PET) cord that runs inside a spacer made of polycarbonate urethane (PCU). When implanted the cords are in 300 N of tension, which secures the screw heads to the PCU spacers and helps restrain flexion. The PET cord is meant to carry tensile loads during flexion and the PCU spacers are intended to resist compressive forces. Unfortunately the

9

compressive loads on the PCU spacers produce bending moments in screws, which may cause screw loosening [31].

The Dynesys was found to have no significant difference when compared to a rigid fixator in flexion [32, 33]. However in extension the Dynesys restored motion comparable to an intact spine segment. In lateral bending the Dynesys was less flexible than the intact spine, with values similar to rigid fixation. In axial rotation the Dynesys appears to have a similar ROM as an intact spine [33]. These results indicate that a spine stabilized with the Dynesys is stiffer than an intact spine. Overall the change in intradiscal pressure was found to be similar between the Dynesys and rigid stabilization [34]. It has also been found that the Dynesys significantly reduces anterior disc height, and even with the device implanted, disc degeneration continues to be a problem [35]. The most common reason for revision of the Dynesys is ASD [10].

One material used as an alternative for titanium for semi-rigid fixation is polyetheretherketone (PEEK). Because PEEK systems are relatively new, studies have been performed on the CD HORIZON LEGACY PEEK Rod to characterize the biomechanical properties of the PEEK system and compare it to lumbar fusion systems [36]. The PEEK rods were developed to provide a semi-rigid fixation system that closely replicates the natural load distribution of the lumbar spine for patients who undergo spinal fusion. PEEK rods have been found to more closely approximate the physiologic anteroposterior column load sharing compared to results with titanium rods.

The Stabilimax NZ is a PDS device that is designed to reduce the neutral zone after spinal surgery while maintaining a natural ROM [37]. The neutral zone is the region of intervertebral motion around a neutral posture. In this position it takes little effort for the muscles to stabilize the spine. Research has shown that degeneration of injury to the spine results in an

initial increase of the neutral zone. Surrounding muscles are required to compensate for a larger neutral zone, which can result in LBP. The Stabilimax NZ is intended to reduce the neutral zone back to natural levels while maintaining ROM. The device is a pedicle screw based system that has dual concentric springs combined with a ball and socket joint. Studies performed on the Stablimax NZ showed that the device placed a smaller load on the bone-screw interface than other systems while maintaining the ROM.

Some other posterior dynamic stabilization devices not specifically discussed here include the Isobar TTL semi-rigid rod, Cosmic Posterior Dynamic System, AccuFlex rod system, and many others [26]. The existence of so many different types of devices suggests an optimal design has yet to be achieved. There is a lot of room for improvement in the design of dynamic stabilization devices, and was a motivating factor in the creation of the FlexSPAR.

2.4.1 The FlexSPAR

The spine has a natural nonlinear force deflection relationship that enables the spine to have passive stability. In a degenerate disc the spine gradually loses passive stability. The FlexSuRe™ [38] is a compliant PDS device [39] that was designed to restore stability through the use of tailorable contact-aided inserts that alter the nonlinear deflection response observed in spinal motion. While the concepts behind the FlexSuRe were promising, it was not designed to share a significant portion of the compressive forces seen from upper body weight, nor was did it have any resistance to axial rotation [38]. Therefore a new device, the FlexSPAR™ (Figure 2-2), was developed using the design principals of the FlexSuRe. The FlexSPAR also uses contact-aided inserts and is a more compact version of the FlexSuRe.

11

Figure 2-2: The FlexSPAR shown implanted with pedicle screws but without the inserts and protective shrouds.

3 FINITE ELEMENT ANALYSIS

Finite element analysis is useful in breaking down a complex problem into many small simple problems. In the current application, finite element models are useful in making variations between models which allow for a direct comparison between different conditions. It is also easy to vary material properties and loading conditions.

3.1 Finite Modeling of the Spine

There is a significant amount of research being done on finite element analysis of the spine. Many of the models are not lumbar spine models, but still have significance in setting the foundation of finite element modeling of the spine.

Zander et al. have developed a L1-L5 and L3-L5 lumbar spine model which have been used to study variations in spinal flexibility, intradiscal pressure, facet contact forces, follower loads, and axial rotations [40-43].

Shirazi-Adl et al. have developed a series of finite element models used to study stresses during compression, lateral bending, and axial rotation [44-46]. One of these models incorporated the surrounding muscles and finding the optimum posture [47].

Goel et al. have developed models of different regions in the spine [48-51]. These models have been used to study interlaminar shear stresses and wear in artificial discs. Ahn et al. have developed a model to compare characteristics between pedicle-based dynamic and rigid rod devices [52].

Schmidt and Wilke et al. have created finite element models to evaluate the relationship between the instantaneous axes of rotation and facet joint stresses, the risk of disc prolapse, and the required axial and bending stiffnesses of posterior implants in the design of a flexible lumbar stabilization system [53-55].

Bowden et al. have created a validated lumbar spine model of an FSU. The material properties of the IVD and ligaments were varied to better predict the quality of motion [56].

Rundell et al. have created a validated L3-L4 spine model used to determine how total disc replacement positioning and nucleus pulposus replacement affect the biomechanics of a motion segment. The models were validated using range of motion, disc pressures, and bony strains from previously published studies [57, 58].

There are a few studies that are particularly relevant in setting the finite element parameters for the current work. One of the challenges associated with modeling the lumbar spine with a PDS device is accurately modeling a degenerative disc. There is little quantitative data available for use on varying grades of degeneration that can be applied to a finite element model. Wilke et al. created a grading system for disc degeneration where height loss was defined for grade 0: 0%, grade 1:0-33%, grade 2: 33-66%, and grade 3: 66-100% [59]. This grading system was used by Schmidt et al. to create a finite element model of a L4-L5 FSU that compared intradiscal pressure and strains between the AF and endplates with varying levels of disc degeneration [55]. This grading system is an effective way to define varying levels of degeneration in a finite element model.

Rohlmann et al. presented studies that helped define parameters for the current work [12, 16, 25, 60]. One of the studies investigated the mechanical effects of disc degeneration on a FSU. The healthy nucleus pulposus was modeled as an incompressible fluid. As a disc degenerates its

14

material properties become similar to the AF, which is compressible. Therefore the bulk modulus of a degenerate disc can be modified to be compressible, with compressibility similar to the AF. One of the shortcomings with Rohlmann's model, however is that it was assumed that disc degeneration had no effect on the material properties of the AF. O'Connell et al. have recently shown that the outer AF material properties are altered with degeneration [19].

The Rohlmann studies also compared the effects of a posterior dynamic stabilization system to a rigid fixation system using a finite element model of an L1-S1 spine segment [25]. The study compared a healthy disc between L3 and L4 with a degenerate disc. Rohlmann concluded that the adjacent segment is only slightly altered by the dynamic implant. While this study has many similarities to the proposed work, there are differences as well. The ligaments in Rohlmann's model are modeled as tension-only spring ligaments, whereas in the current work the ligaments are modeled as shell elements. In addition, the pedicle screws were represented as beam elements rather than hexahedral elements. The study also did not use an actual PDS device, but simply altered the stiffness of longitudinal rods to compare the difference between a rigid fixation system and dynamic stabilization device. Finally, the study did not evaluate the influence of a decompressive pre-load on a posterior dynamic stabilization device.

3.2   Methods

Five different models were tested and compared. The first model was tested assuming an uninstrumented spine segment with a healthy disc. The healthy nucleus pulposus was considered to be nearly incompressible, and was modeled using elastic fluid elements [16]. The model was then modified to simulate a Thompson scale grade 1 degenerate disc at the L3-L4 level. Four situations were tested with a degenerated disc at L3-L4: without instrumentation, with a FlexSPAR at L3-L4 that had an intrinsic decompressive pre-load, a FlexSPAR without a pre-

15

load, and with bilateral rigid fixators. The degenerate disc was modeled by modifying the bulk

modulus of the nucleus pulposus and applying compression to the model until disc height was

reduced by 16.5%, which is the mid value of grade 1 degeneration reported in literature [16, 59].

The material properties of the outer annulus fibrosus have been found to change with

degeneration, and those changes were incorporated into the degenerate disc model as well [19].

The pre-load for the FlexSPAR was accomplished by axially compressing the FlexSPAR 2 mm

(Figure 3-1) and then inserting it into the spine model with initial pre-stresses and strains. During

application of the follower load, which represents the compressive forces resulting from upper-

body weight, the stresses in the FlexSPAR relax. This resulted in a spring-like behavior where

the FlexSPAR "unwinds" and the disc is distracted.
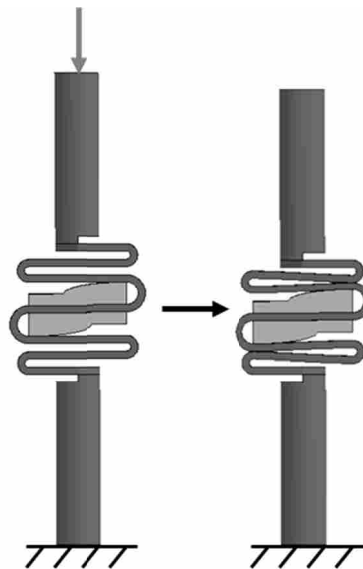
Figure 3-1: Applying a pre-load to the FlexSPAR

The L3-L4 level of the model was "virtually" implanted with pedicle screws which were

connected by a finite element model of the spine instrumentation. Since the model was intended

to simulate spinal biomechanics after healing, the bone-screw interface was considered to be

permanently bonded together. The L3-L4 level of implantation was chosen so that the effects at the adjacent levels could be studied if desired.

3.2.1   Vertebrae

The vertebral geometry was created obtained from quantitative computed tomography (QCT) scans of a cadaveric 65 year-old female. Using QCT scans is a common method for generating the geometry of the bony surfaces [16, 51, 57, 61]. The spine geometry was segmented from the QCT data using Anaylze (Version 8.0, Mayo Clinic, Rochester, MN). The geometry of the intervertebral discs and other individual spine components were created using thresholded QCT data.

Different material properties were assigned for the cortical and cancellous bone. The bone mineral densities in the cancellous bone can be correlated to the accompanying CT Hounsfield unit from the scan. This was accomplished by assigning unique bone mineral density values at each node in the mesh using custom computer code that correlated CT voxel intensity with the bone mineral density. With the data from the QCT scans, the anisotropic tissue moduli of the cancellous bone was determined through the use of experimental relationships reported by Morgan et al. and Ulrich et al. [62, 63]. The cortical bone on the vertebral surfaces was modeled using shell elements due to a variation in QCT threshold values along the edge surfaces. The cortical bone was assumed to have homogeneous isotropic material properties [51, 64]. The contact between the facets of each vertebral body was modeled as a non-friction surface-to-surface penalty method.

3.2.2   Intervertebral Disc

The intervertebral disc was split into three sections in the model: the inner and outer annulus fibrosus and the nucleus pulposus. The annulus fibrosus was modeled with transverse orthotropic elastic properties. It was split into two different sections to account for a difference in mechanical behavior through the thickness of the annulus fibrosus [65]. The nucleus pulposus, which makes up about 40-50% of the disc was considered to be nearly incompressible, and was modeled using elastic fluid elements [16, 25]. A slightly degenerated nucleus pulposus was modeled by modifying the bulk modulus of the nucleus pulposus until disc height was reduced by 16.5%, which is the mid value of grade 1 degeneration reported in literature [16, 59]. The material properties of the outer annulus fibrosus have been found to change with degeneration, and these changes were incorporated into the degenerate disc model [19].

3.2.3   Ligaments

Many finite element models use nonlinear spring elements for representing spinal ligaments [25, 40, 51, 52, 54, 66, 67]. These elements can mimic spinal flexibility, but do not account for the shear forces in the ligaments, material anisotropy, and interactions that may occur between ligaments. Spinal ligaments in this model were represented as nonlinear, tension-only fabric shell elements. This type of element allows for loading in tension and shear, but not compression. The material properties defining the ligaments were taken from literature [56, 68].

3.3   Loading Conditions

The finite element models were tested in flexion (+8 Nm), extension (-6 Nm), bilateral bending (±6 Nm), and bilateral axial rotation (±6 Nm) using LS-Dyna (Version 971 R5.1.1, LSTC, Livermore, CA). The loading directions are shown in Figure 3-2. A 444 N compressive

follower load was applied to simulate upper body weight and muscular loads. A follower load runs tangent to the spinal surfaces and follows the lordotic curvature of the spine [69]. The follower load is intended to mimic the *in vivo* physiologic compressive loads seen in the lumbar spine.
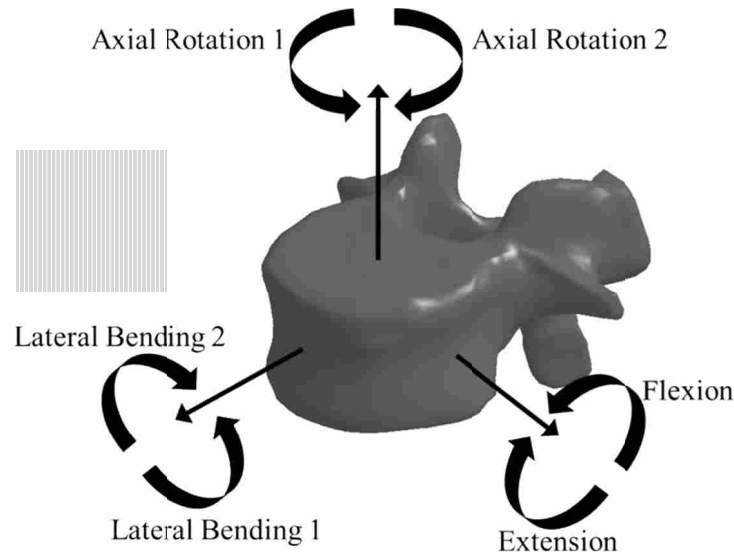
Figure 3-2: Loading directions

3.4 Validation

The proper mesh density needed for this model to accurately predict spinal behavior was verified [70]. Stress convergence between two models, one with double the elements of the other, were within 5% of each other. The model consisted of 234,429 nodes and 243,441 elements. The model was validated by comparing its behavior to experimental data, including range of motion, quality of motion, intradiscal pressures, disc degeneration, cortical strains, and instantaneous axes of rotation.

3.4.1 Range of Motion

The ROM was validated by comparing kinematic data from the model to experimental data found in literature (Figure 3-3) [24, 71-73]. Kinematic data from the model was collected by fixing S1 and applying loading moments at T12 in flexion/extension, lateral bending, and axial rotation.
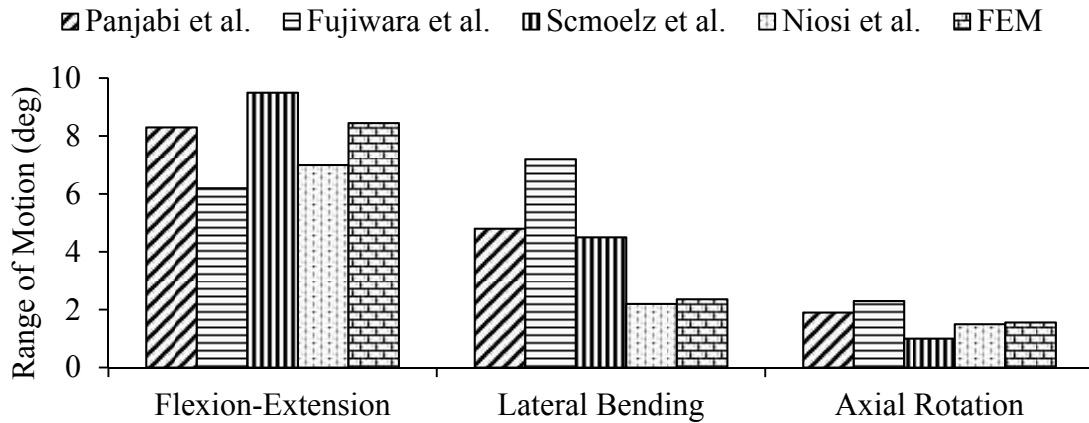
Figure 3-3: Range of motion validation

3.4.2 Quality of Motion

Quality of motion, which is the applied moment versus angular displacement, was checked to verify that the model followed a nonlinear path as presented in literature [56]. Figure 3-4 displays the range of motion and quality of motion of an intact L3-L4 FSU.
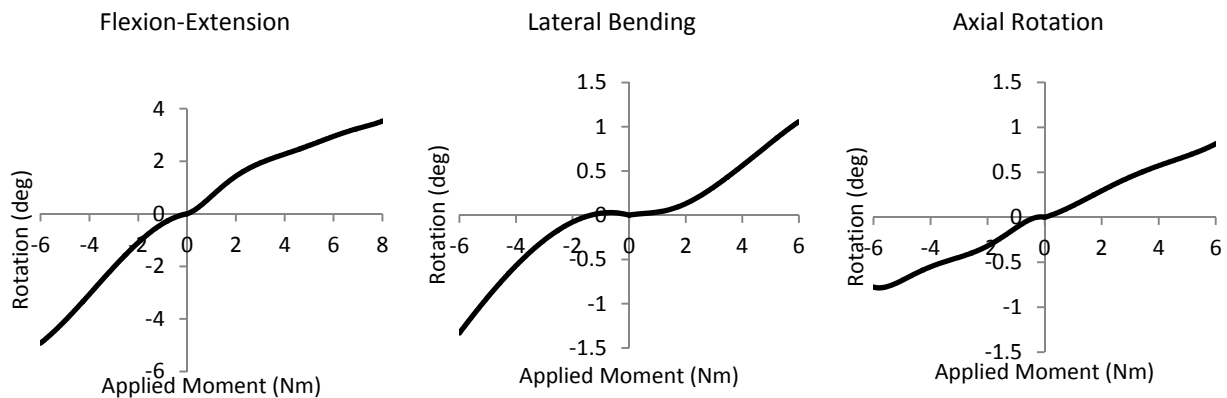
Figure 3-4: Quality and range of motion of an L3-L4 FSU

20

3.4.3 Disc Pressures

The intradiscal disc pressures were validated by averaging the disc pressures in the center of the nucleus pulposes in the finite element model to data presented in literature [74]. The averaged pressures in the model simulated the experimental data collected by probes. The data presented in literature (Figure 3-5) was compared against the compression results from the model (Figure 3-6).
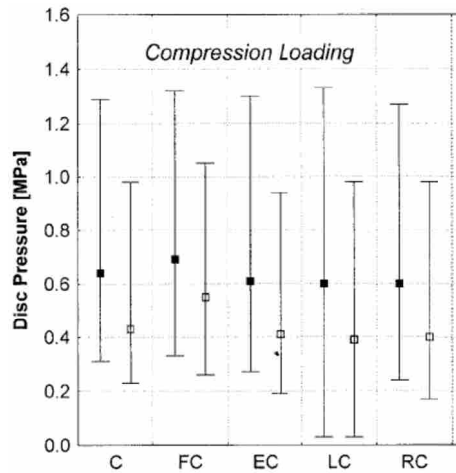
Figure 3-5: Disc pressure data from Frei et al.
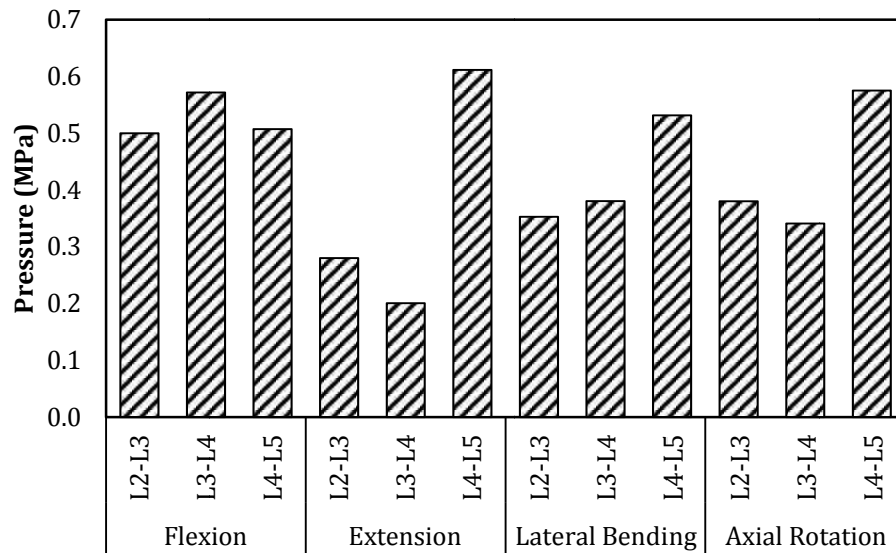
Figure 3-6: Disc pressures obtained from the model

3.4.4   Disc Degeneration

Disc degeneration at L3-L4 was validated by comparing disc heights of a healthy disc and a slightly degenerated disc. Wilke et al. created a quantitative grading system of different levels of degeneration [59]. A grade 1 disc was considered to correspond with a disc height reduction of 0-33%. A mildly degenerated disc was defined as having a disc height reduction of approximately 16.5%, which is the mid value for a Grade 1 degenerated disc as defined by Wilke et al. To model a reduction in disc height, the bulk modulus of the L3-L4 disc was modified and compression on the disc was applied until disc height reduction fell to approximately 16.5%. Per Wilke's protocol, to measure the height loss, the anterior and posterior edges of the vertebral body are defined as those points having the largest distance to the center of the vertebral body. The perpendicular distance from the midplane of the disc to the edges of the vertebral body was then measured. The sum of the distances was defined as actual anterior height and posterior height. Figure 3-7 compared the anterior and posterior disc height reduction for a healthy and slightly degenerated disc. Height measurements were performed by importing the images into Matlab and measuring the distances between points. The measurements were calibrated via a 1 mm box placed in the images.

| (a) Healthy | (b) Degenerate |
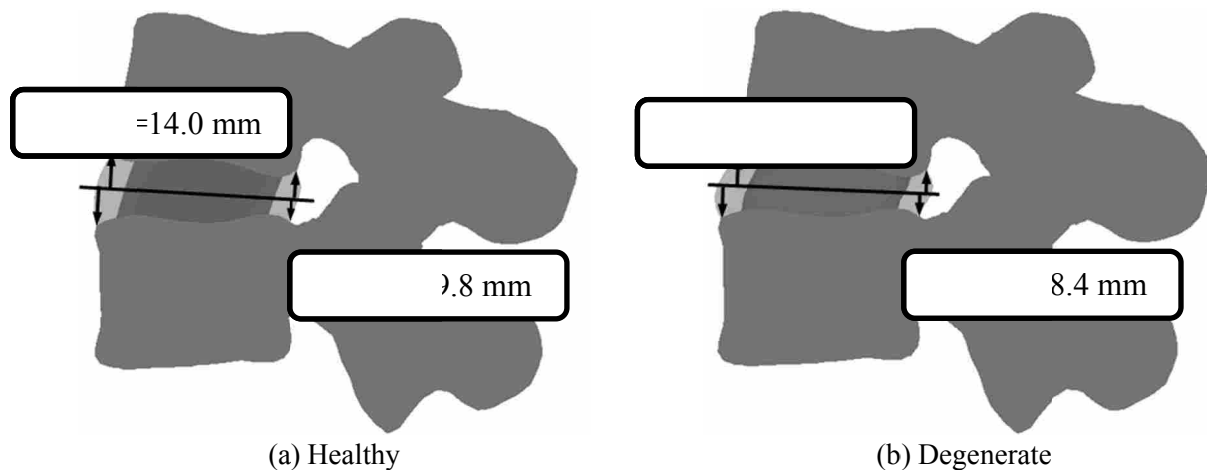
Figure 3-7: Validation of disc height reduction

3.4.5 Instantaneous Axes of Rotation

The instantaneous axes of rotation (Figure 3-8) for each functional spinal unit was calculated and compared to the location of the axes of rotation shown in Figure 3-9 and [75].

Figure 3-8: Location of axes of rotation
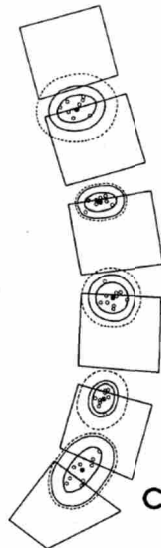
Figure 3-9: Location of axes of rotation from Pearcy et al.

3.4.6   Cortical Strains

A separate finite element model was used to validate the cortical strains previously reported [74]. In the previously reported study a 1000 N follower load was applied and cortical strains were measured. Cortical strains were validated by creating a finite element model with a 1000 N follower load and then comparing the first principal strains in the finite element model to the experimental values found at seven different locations of a vertebral body. Table 3-1 displays the first principal strains found in literature and in the model.

Table 3-1: Cortical strains (microstrain)

Location	Lower Limit	Upper Limit	Model
Anterior Endplate	177	3168	1110
Posterior Endplate	464	2032	1159
Left Endplate	137	4497	895
Right Endplate	273	2548	593
Right Rim	215	463	388
Anterior Rim	431	916	716
Left Rim	192	711	538

3.5   Summary

There are many different techniques used in computer modeling of the human spine. In this work, a finite element model of the lumbar spine was extensively validated using published literature, and stress convergence was verified. The model exhibited good quality of motion, which is the nonlinear path a spine segment follows during movement. A method for modeling disc degeneration was developed and explained. Additionally, one method of applying a decompressive pre-load to the FlexSPAR was determined.

Due to the complexity of finite element models, they can be sensitive to changes in the boundary conditions or material properties. The bulk of the properties applied to the present model have already been investigated using a sensitivity study [56]. In the present work, the

positional sensitivity of the follower load within the model was observed. To minimize this sensitivity, the position of the follower load was varied until the center of rotation of the model did not change with follower load location. Additionally, an analysis was performed to determine whether there was a large effect in varying the number of points found in the model that relate the experimental relationship between cancellous bone density and modulus [63]. Two separate models were compared; one with only a few points defining cancellous bone properties, and another with more than five times the amount of points. After direct comparison it was determined that there was little difference whether more data points were used to define the cancellous bone material properties.

4   BIOMECHANICAL EFFECTS OF THE FLEXSPAR

4.1   Introduction

Posterior dynamic stabilization (PDS) devices were introduced to the U.S. market several years ago as an alternative to spinal fusion, which is a common method of treatment for painful degenerative disc conditions [76]. PDS devices are intended for patients with chronic low back pain who have early stage disc degeneration. Disc degeneration is often thought to be the source of low back pain and over 90% of all surgical interventions in the spine are performed due to degenerative disc conditions [2]. The goal of a PDS device is to mechanically stabilize the degenerated spinal segment while restoring, at least partially, the motion of a healthy spine segment [11, 77, 78]. PDS devices share load with the intervertebral disc and facet joints, acting as an internal brace, which allows the spine to move while restricting motion extremes that are more likely to mechanically trigger pain [11, 78]. The purpose of this study was to evaluate the influence of an intrinsic decompressive pre-load on a PDS on the biomechanical response of the lumbar spine.

The intervertebral disc is an avascular tissue that receives its nutrients through diffusion and bulk fluid flow [2]. If the diffusion process is disturbed, nutrition content drops. Disc degeneration begins when the loss of matrix proteins exceeds the creation or retention of them in the disc [2]. This leads to a decrease in proteoglycan concentration, and a gradual change of the collagen tissue to a more fibrous tissue [15]. Desiccation of the intervertebral disc leads to an

inability of the nucleus pulposus to transmit weight and exert pressure radially on the annulus fibrosus, leading to disc height reduction and posterior-lateral bulging of the intervertebral disc [16]. Additionally, disc degeneration alters the spine segment's motion [79], intradiscal pressures, and load sharing, which leads to mechanical instability and pain [2]. Dynamic stabilization devices are intended to address these changes by reducing loading on a compressed disc and improving the post-operative motion to match healthy intersegmental motion [12]. These outcomes are presumed to increase spinal stability without transferring additional stress to adjacent segments [13].

It has been posed that the effectiveness of PDS devices could be increased if the devices themselves were pre-loaded such that after insertion the device could counteract the compressive forces resulting from upper body weight [28, 38]. A recently developed dynamic stabilization device (the FlexSPAR™) which supports this ability was used as a test case. The decompressive pre-load was added to the device by axially compressing it and then inserting it into the model. The study utilized a nonlinear finite element analysis approach to provide the ability to more closely examine load-sharing, mechanical stress, adjacent level effects and vertebral bone strain energy. The hypothesis of this study was that pre-loading a PDS would increase disc height and improve segmental biomechanics.

4.2   Methods and Materials

The FlexSPAR™ (Figure 4-1), referred to henceforth as the PDS, is a compliant device with a tailorable nonlinear force-deflection response [39, 56]. The design of the device evolved from an earlier version, the FlexSuRe™, and was designed to be a more compact version of the original design. [38]. Because healthy motion varies between individuals [80], the device can be

customized through the use of contact-aided inserts that alter its force-deflection relationship. The inserts allow the device to have a tailored range of flexibility or stiffness, depending on the needs of the patient.

Figure 4-1: The FlexSPAR shown implanted with pedicle screws and without the inserts and protective shrouds.

4.2.1 Finite Element Model

A three-dimensional hexahedral finite element model of a L1-L5 ligamentous lumbar spine segment was created using QCT data from a 65 year old female cadaveric spine (Figure 4-2). The spine geometry was segmented from the QCT data using Analyze (Version 8.0, Mayo Clinic, Rochester, MN). The geometry of the intervertebral discs and other individual spine components were created using thresholded QCT data.
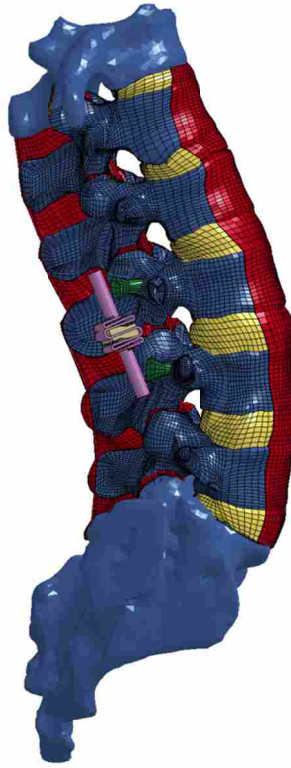
Figure 4-2: Hexahedral model of the instrumented lumbar spine

The bone mineral densities in the cancellous bone were correlated to the accompanying CT Hounsfield unit from the QCT scan. This was accomplished by assigning unique bone mineral density values at each node in the mesh based on calibrated CT voxel intensity. Anisotropic tissue moduli of the cancellous bone were determined through the use of experimental relationships reported by Morgan et al. [63] and Ulrich et al. [62]. The cortical bone on the vertebral surfaces was modeled using shell elements with homogeneous and isotropic material properties [51, 64]. The contact between the facets of each vertebral body was modeled as a non-friction surface-to-surface penalty method.

The L3-L4 level of the model was "virtually" implanted with pedicle screws which were connected to a finite element model of the spinal instrumentation. Since the model was intended

to simulate spinal biomechanics after healing, the bone-screw interface was considered to be permanently bonded together. Additionally the screws were considered to be unthreaded to add simplicity to the model [25, 52, 66, 81]. The L3-L4 level of implantation was chosen so that the effects at the adjacent levels could be studied.

Five different models of the spine segment were tested and compared:

- Uninstrumented with a healthy (intact) disc.

- Unistrumented with a degenerate disc.

- Instrumented with the PDS that had an intrinsic decompressive pre-load.

- Instrumented with the PDS without a decompressive pre-load.

- Instrumented with bilateral rigid fixators.

In the healthy model the nucleus pulposus was considered to be nearly incompressible, and was modeled using elastic fluid elements [16]. The model was then modified to simulate a Thompson scale grade 1 degenerate disc at the L3-L4 level. The degenerate disc was modeled by modifying the bulk modulus of the nucleus pulposus and applying compression to the model until the disc height was reduced by 16.5%, which is the mid value of grade 1 degeneration reported in literature [16, 59]. The material properties of the outer annulus fibrosus have been found to change with degeneration, and those changes were incorporated into the degenerate disc model as well [19]. The decompressive pre-load for the PDS was accomplished by axially compressing the PDS by 2 mm and then inserting it while pre-stressed into the spine model. During application of the follower load [69], which simulates upper body weight, the stresses in the PDS relax. This resulted in a spring-like behavior where the PDS "unwinds" and the disc is distracted. Table 4-1 and

Table 4-2 summarizes the material properties in the model.

31

Table 4-1: Material properties

Structure	Formulation	Modulus (MPa)	Poisson's ratio	References
Cortical bone	Isotropic, elastic shell elements	12000	0.2	[51, 64]
Cancellous bone	Density dependent anisotropic, elastic hex elements	$E_z=4730\rho^{1.56}$ (a) $E_x=0.42E_z$ $E_y=0.29E_z$	0.23, 0.4, 0.38 (b)	[62, 63]
Inner annulus fibrosus	Anisotropic, elastic hex elements	5.59,0.34,0.19 (c)	1.86,0.88,0.14 (c)	[65]
Outer annulus fibrosus (healthy)	Anisotropic, elastic hex elements	20.9,0.42,0.29 (c)	2.27,0.79,0.61 (c)	[19]
Outer annulus fibrosus (degenerate)	Anisotropic, elastic hex elements	22.9,0.32,0.35 (c)	1.88,0.46,0.61(c)	[19]
Pedicle Screws (titanium)	Isotropic, hex elements	113800	0.342	[25]
FlexSPAR (titanium)	Isotropic, hex elements	113800	0.342	[38]
Rigid Fixators (titanium)	Isotropic, hex elements	113800	0.342	[25]

* (a) The modulus in the Z direction represents the axial direction and is calculated from the bone mineral density. The moduli ratios in the orthogonal directions were obtained from literature. (b) Poisson's ratios for the three orthotropic directions. (c) Orthotropic moduli and ratios.

Table 4-2: Nucleus pulposus material properties

Structure	Formulation	Bulk Modulus (MPa)	References
Nucleus pulposus (Grade 0)	Fluid, hex elements	1720	[59, 82]
Nucleus pulposus (Grade 1)	Fluid, hex elements	70	[16, 59]

The spinal ligaments were represented using nonlinear, tension only, fabric shell elements [83]. The major spinal ligaments represented were: anterior longitudinal ligament (ALL), posterior longitudinal ligament (PLL), ligamentum flavum (LF), interspinous ligament (ISL), supraspinous ligament (SSL), and the capsular ligament (CL). Cross-sectional areas from literature were assigned to the shell elements representing ligaments [68]. The properties for the CL were simplified to be linear. The nonlinear constitutive material properties were applied to each ligament and applied as piecewise linear functions as shown in Table 4-3.

Table 4-3: Ligament properties

Ligament	Cross-sectional area	Constitutive relationship - strain, stress [a]		
		A	B	C
ALL	65.6 mm^2	0.12, 1.15	0.44, 9.11	0.57, 10.3
PLL	25.7 mm^2	0.11, 2.04	0.34, 16.19	0.44, 20.8
LF	39.0 mm^2	0.07, 2.04	0.19, 9.14	0.25, 10.38
ISL	15.1 mm^2	0.17, 0.95	0.38, 5.86	0.54, 6.69
SSL	15.1 mm^2	0.17, 0.95	0.38, 5.86	0.54, 6.69
CL	0.074 mm[b]	E=0.3 [c]		
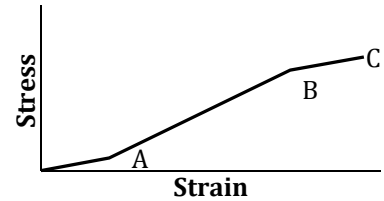
*NOTE (a) The relationships for the all of the ligaments except for the facet joint capsules were modeled using three linear regions. The modulus changes at points A, B, and C, which are listed for each ligament as the stress-strain relationship. (b) The ligament size for the CL is reported as thickness. (c) The facet joint capsules were simplified as linear elastic with the stated modulus.

4.2.2   Verification and Validation

Stress convergence of the finite element mesh density was verified [70] and the model was validated (see Chapter 2 for more detail) by comparing its behavior to experimental data, including range of motion (ROM) [71], quality of motion [56], intradiscal pressures [74], instantaneous axes of rotation [75], and cortical strains [74]. Disc degeneration at L3-L4 was validated by comparing disc heights of a healthy disc and a slightly degenerated disc. A grade 1 disc has been reported to correspond with a disc height reduction of 0-33% [59]. The model exhibited a height reduction at the degenerated level of approximately 16.5%, which is the mid-range value for a Grade 1 degenerated disc.

4.2.3   Testing Method

The finite element models were tested in flexion (8 Nm), extension (6 Nm), bilateral bending (±6 Nm), and bilateral axial rotation (±6 Nm). A 444 N compressive follower load was applied [69] to simulate upper body weight and muscular loads. The sacral interface was fixed

from translation and rotation and pure moment loads were applied to T12. Because of the nonlinearity and complexity of the models, finite element analysis was conducted using LS-Dyna (Version 971 R5.1.1, LSTC, Livermore, CA) using the resources of the Fulton Supercomputing Center at Brigham Young University. A total of 30 nonlinear finite element simulations were performed. Each finite element simulation required approximately 1200 CPU hours on a hex-core Intel Westmere (2.67 GHz) workstation with 24 GB of core memory.

Disc pressures, load sharing, ROM, instantaneous axes of rotation, and strain energy were measured for a direct comparison between each loading condition. The disc pressures were determined by averaging the disc pressures in the center of the nucleus pulposes. The facet contact forces were determined by summing the interface forces at each node in the facet joints. Change in ROM was determined by measuring the change in angle between the superior and inferior endplates of each FSU in the spine segment. The bone remodeling stimulus was computed at each node by measuring the change in strain energy density (SED) between the degenerate and implanted models as [84]:

$$\% \, Change = \frac{SED_{implanted} - SED_{degen}}{SED_{degen}} \tag{4-1}$$

Kerner et al. have defined a 75% change in strain energy as the threshold where a change in bone architecture is likely to occur [85]. Areas with changes above 75% were designated areas of bone formation, and changes below -75% were designated areas of bone resorption.

4.3 Results

Disc degeneration resulted in a decrease in disc pressure during flexion, extension, and lateral bending (Figure 4-3). Rigid fixators further decreased disc pressures for all loading

conditions. The PDS with and without the pre-load behaved similarly: they improved disc pressures in comparison to rigid fixators but did not restore the disc pressure to healthy levels.
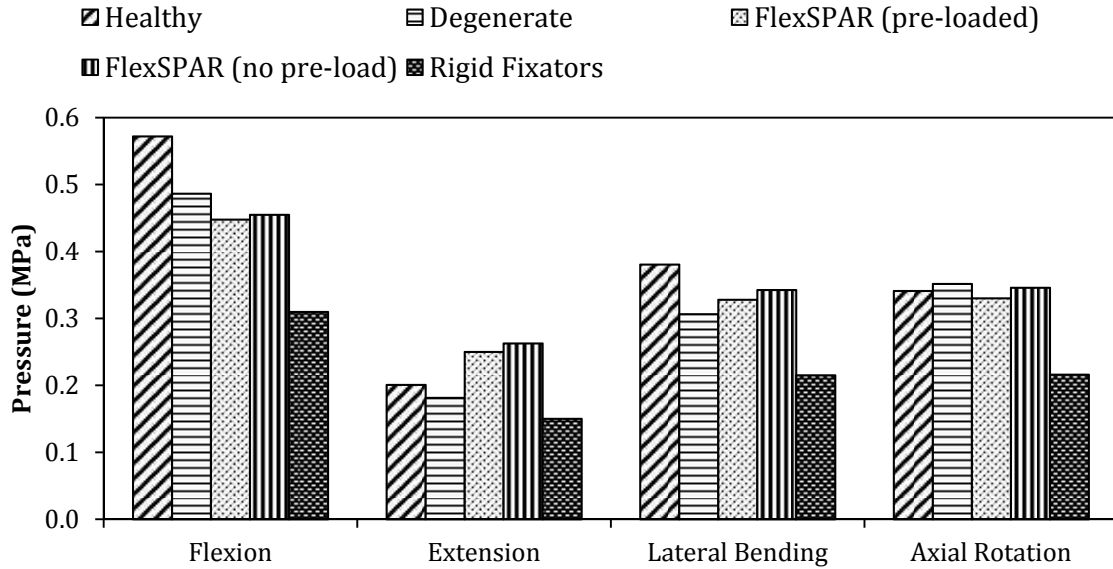
Figure 4-3: Intervertebral disc pressures shown at the surgical level (L3-L4) for all loading conditions

Consistent with previously published results, degeneration increased segmental ROM in flexion-extension, lateral bending, and axial rotation [16, 73] (Figure 4-4). The rigid fixators significantly reduced the ROM (beyond the healthy condition) for all loading directions. The PDS reduced the ROM, approaching that of the healthy condition. In flexion/extension the pre-loaded PDS resulted in a smaller ROM than the PDS without a pre-load. This indicated that the pre-loaded PDS was too rigid in the sagittal plane. In lateral bending the pre-loaded PDS resulted in a better ROM in comparison to the PDS without a pre-load. In axial rotation there was little difference between the PDS with and without a pre-load.
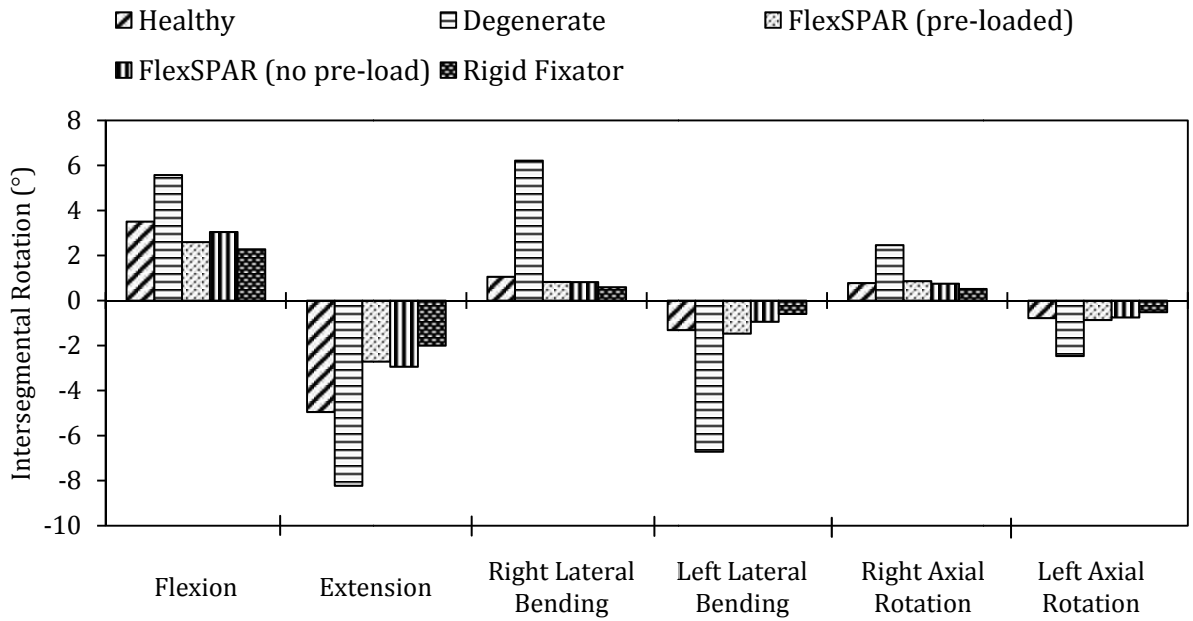
Figure 4-4: Range of motion of the L3-L4 FSU (all test cases)

Spinal instrumentation shifted the flexion-extension axis of rotation posteriorly as compared to the healthy condition (Figure 4-5). Rigid fixators resulted in the most extreme posterior translation. The axis of rotation for the pre-loaded PDS was slightly more posterior than the axis for the PDS without a pre-load.
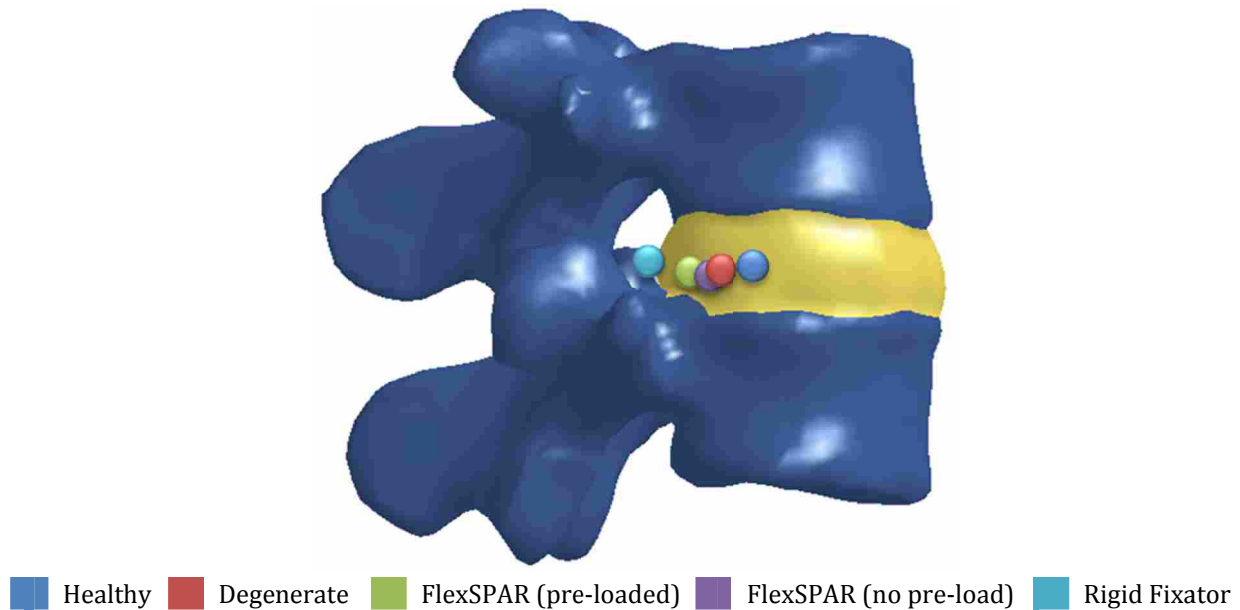
Figure 4-5: Change in helical axes at L3-L4

The degenerate case demonstrated a large increase in facet contact forces as compared to the healthy case (Figure 4-6). The pre-loaded PDS and rigid fixators distracted the facet joints, which eliminated facet contact forces at the operated level (L3-L4). None of the instrumentation sets resulted in large changes in facet contact force at the adjacent levels.
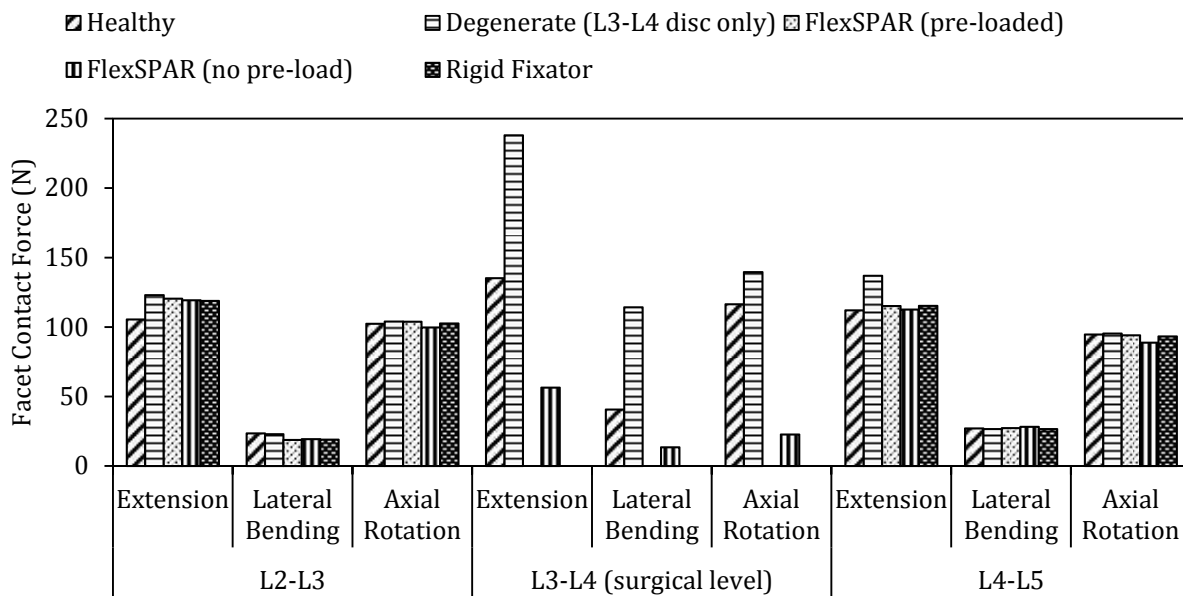
Figure 4-6: Facet contact forces

Restoring disc height is thought to be an important factor in restoring the biomechanics of an unstable spine [86, 87]. Table 4-4 displays the changes in disc height at the anterior and posterior regions of the disc. The pre-loaded PDS distracted the posterior disc in comparison to the degenerate condition, but did not substantially distract the anterior disc. As expected, neither of the other instrumented conditions (rigid fixator, no pre-load PDS) resulted in changes to the intervertebral disc height.

Table 4-4: Intervertebral disc heights

	Intact	Degenerate	PDS (pre-loaded)	PDS (no pre-load)	Rigid Fixators
Anterior Height (mm)	14.0	11.8	12.0	11.8	11.8
Posterior Height (mm)	9.8	8.4	9.0	8.4	8.4

The addition of spinal instrumentation resulted in changes in vertebral bone strain energy (Figure 4-7). Changes in bone strain energy have been associated with bone remodeling stimulus [57, 70, 77], but there is not yet a strong validation of this correlation. During flexion there were minimal changes in bone remodeling stimulus after implantation of a pre-loaded PDS. Conversely, the bone remodeling stimulus predicted regions of bone resorption after implantation of the rigid fixators and the PDS without a decompressive pre-load. During extension, bone formation was generally predicted to occur at the anterior-superior region of the L4 vertebral body. Additionally, bone resorption was predicted to occur at the facet joint.

Load sharing between the various elements of the model at the treated level (L3-L4) was altered for each test case. Note that while the overall loading on the spine is compressive, certain elements (notably the ligaments, and in some cases the instrumentation) experience tensile loading (Figure 4-8). In flexion, the segment with a PDS experienced about a 10% increase in load sharing in the disc, whereas the rigid fixators reduced disc load sharing by about 10%. In extension, the PDS reduced disc load sharing by about 10% while the rigid fixators reduced disc load sharing by 30%. The pre-loaded PDS shared 5% more of the load than the PDS without a pre-load. The rigid fixators shared more than twice the compressive loads as compared with the PDS.

FlexSPAR (pre-loaded)   FlexSPAR (no pre-load)   Rigid Fixators

Flexion

Extension

Resorption   Formation
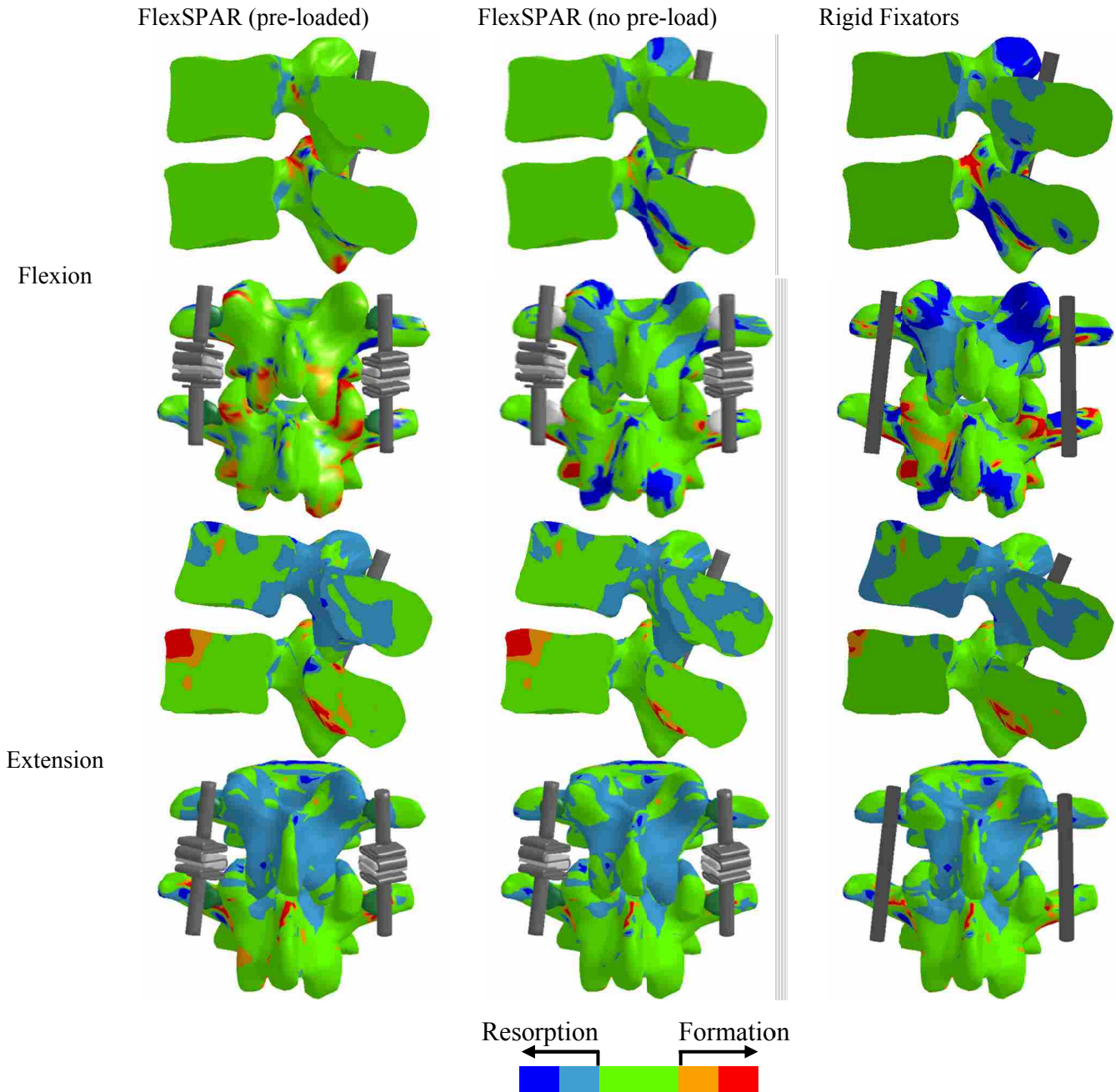
Figure 4-7: Changes in vertebral strain energy (bone remodeling stimulus) in the L3-L4 segment as compared to the degenerate spine simulation. The vertebrae are shown cut through the sagittal plane and from a posterior view.
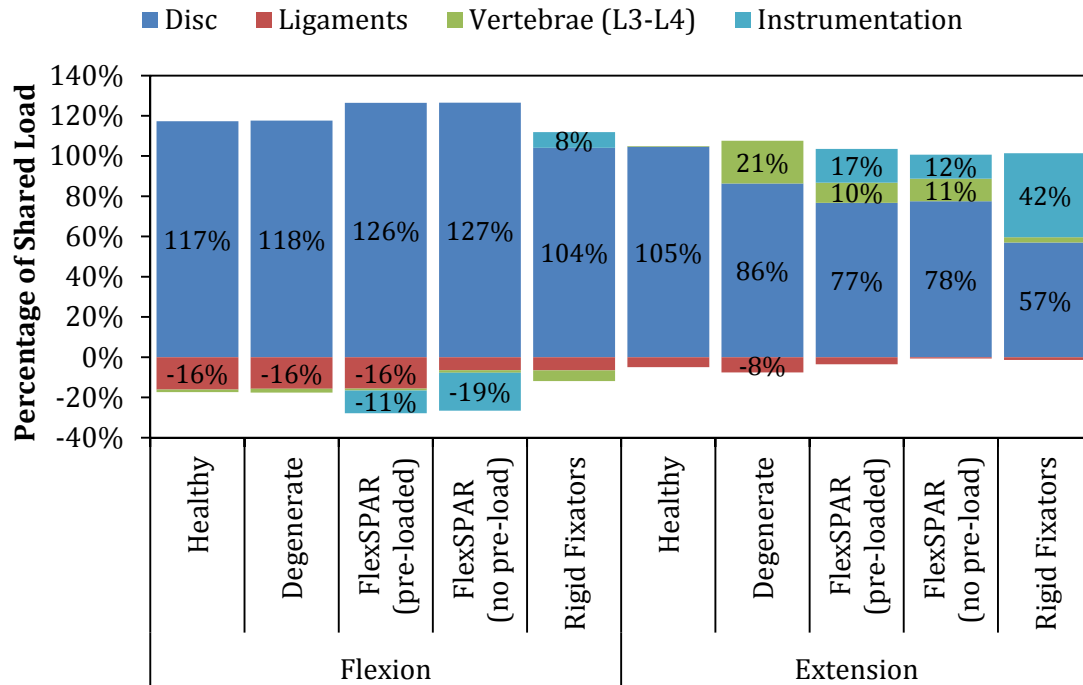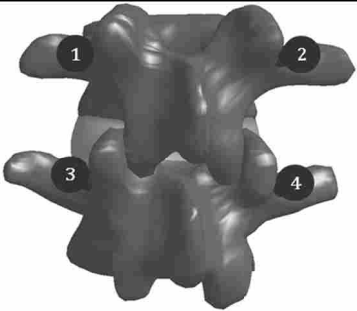
Figure 4-8: Percentage of shared load at L3-L4. Negative percentages represent loads that are opposite the applied compressive follower load. Positive loads are in compression (primary direction of loading) and negative loads are in tension.

Pedicle screws in a rigid fixation system share a majority of the bending and torsion loads at the bone-screw interface until fusion occurs. In contrast, a dynamic stabilization system must withstand these loads indefinitely. Although there is not a specific standard for maximum torque loads applied through the pedicle screws, we have reported a comparison of these loads between the rigid fixators and the PDS. Both the magnitude of the maximum torque loads carried by the screws, as well as the location of the screw experiencing that load was reported. The rigid fixators resulted in the maximum pedicle screw bending moments and torque during every loading condition (Table 4-5,Table 4-6). The PDS significantly decreased these loads in comparison. In general the screws associated with the PDS without a pre-load had smaller bending loads than the pre-loaded PDS. There was little difference between each PDS during torsion.

Table 4-5: Maximum bone-screw bending moment (N-mm) reported for the screw with the largest bending moment.

	FlexSPAR (Pre-Loaded)	FlexSPAR (No Pre-Load)	Rigid Fixators	Pedicle Screws
Flexion	0.68	0.88	2.60	
Extension	0.51	0.28	0.86	
Lateral Bending	0.60	0.53	1.86	
Axial Rotation	0.76	0.71	2.16	
Screw	1	3	3	

The addition of the PDS resulted in smaller loading in torsion in comparison the rigid fixators. In flexion the PDS with a pre-load had a larger load in torsion than the PDS without a pre-load. There was little difference in torsional screw loads in all other loading conditions.

Table 4-6: Maximum bone-screw torsion (N-mm)

Instrumentation	Flexion	Screw	Extension	Screw	Lateral Bending	Screw	Axial Rotation	Screw
FlexSPAR (Pre-Loaded)	0.36	1	0.15	1	0.31	1	0.80	1
FlexSPAR (No Pre-Load)	0.28	3	0.19	4	0.32	2	0.82	2
Rigid Fixators	1.45	3	0.38	2	1.24	2	1.18	3

4.4 Discussion

Posterior dynamic stabilization devices are intended to eliminate mechanical low back pain by reducing loading on a compressed disc and improving post-operative ROM [12]. The proposed modification of these devices to include a decompressive pre-load has been hypothesized to further improve biomechanical function through restoring disc height and segmental biomechanics.

Our results demonstrated that implantation of a PDS accomplished several desirable mechanical outcomes including restoring disc pressures, ROM and the axis of rotation of the degenerated spinal segment to values approaching those of a healthy spinal segment. These improvements were substantially improved as compared to the test case of rigid fixators. Pre-loading the PDS also improved disc height restoration in comparison to the rigid fixators and the PDS without a pre-load. We found that there was little difference in disc pressures regardless of whether a pre-load was applied to the PDS. Additionally, the pre-loaded PDS resulted in an axis of rotation that was slightly posterior to the PDS without a pre-load.

We also compared how spinal instrumentation affected the strain energy (bone remodeling stimulus) in the cancellous bone (as compared to the degenerate condition). Rigid fixation resulted in the most severe changes in strain energy in both flexion and extension, the facets being an area of specific concern. The non pre-loaded PDS exhibited improved (fewer changes) strain energy results as compared to rigid fixation, however there were still substantial indicators that some bone remodeling would likely occur. During flexion we found that each PDS test case was loaded in tension along with the ligaments, while the rigid fixators were loaded in compression (Figure 4-8). Extreme changes in strain energy with the rigid fixators may be due to the instrumentation preventing natural flexion from occurring. Finally, the pre-loaded PDS virtually eliminated strain energy changes in the vertebral bone during flexion, while demonstrating similar results to the other instrumentation in extension. Note that decreases in strain energy (bone resorption stimuli) are generally of more concern than increases in strain energy.

It has been posed that better load sharing will result in reduction of loads in the pedicle screws[88]. Our results indicate that the pedicle screws with the rigid fixators experience greater

loading in bending and torsion at the bone-screw interface in comparison to the PDS. Pre-loading the PDS did not have a significant effect on reducing bending in the screws in comparison to the PDS without a pre-load. However it did result in reduced torsion during extension, lateral bending, and axial rotation.

One of the limitations of the present work is that we examined a single mode of PDS pre-loading. There are several alternative approaches that could have been applied, including applying a larger or smaller compressive pre-load, or including a pre-torque to the device. Our decision here was guided by the observed disc compression due to degeneration, as well as the design geometry of the specific PDS evaluated.

While implications of a PDS device with a pre-load are promising, there are design issues that still need to be addressed prior to widespread adoption of this concept. Stress-relaxation in a device with a decompressive pre-load should be considered. If this is not accounted for the device may eventually behave differently than originally intended. Additionally, after observing the reactions of the model as a result of the applied decompressive pre-load, we feel that the addition of a pre-torque would likely keep the facet joint in contact and evenly distract the disc across the anterior and posterior region. Keeping some degree of contact at the facets would reduce the bone resorption potential at that location. As the parameters for the decompressive pre-load are refined, PDS devices could improve disc height restoration and the segmental biomechanics of the affected level, potentially leading to superior patient outcomes.

5 CONCLUSIONS

This research shows the potential advantages of incorporating a decompressive pre-load into a PDS device. The effectiveness of PDS devices may be improved if the devices themselves carry a pre-load that can counteract the compressive forces resulting from upper body weight [28, 38]. The FlexSPAR, which has the ability to support a pre-load, was used as a test case to determine the potential benefits of using a pre-load in a PDS device. Adding a pre-load to the FlexSPAR generally resulted in improved segmental biomechanics and a decreased likelihood for changes in bone remodeling stimulus.

This research may be used in the future development of PDS devices that improve short and long term performance. Applying a pre-load to PDS devices could play a significant role in the biomechanics of these devices.

5.1 Summary of Contributions

The primary contributions of this work are:

- The development of a finite element model that included the effects disc degeneration.

- Disc height restoration is improved when using a pre-load in the device.

- Application of a pre-load to the FlexSPAR improved ROM and QOM at the affected level.

- A pre-load on the FlexSPAR led to fewer changes in SED which indicates a smaller potential for changes in bone remodeling stimulus.

5.2 Future Work

The results of this study indicate a promising method for improving PDS devices which will hopefully help to alleviate LBP. This study was limited to testing a pre-load on the FlexSPAR by axial compression only. While this was a reasonable method there are other configurations that may warrant investigation. A proposed alternative method of applying a pre-load would be to apply an initial torque on the device along with axial compression. The results from this study indicate that the FlexSPAR applies a moment on the spine segment, resulting in unequal disc distraction at the anterior and posterior regions of the disc. If an initial torque is applied to the device it may counteract the internal moment the device places on the spine segment. If the device itself is able to carry an internal moment it may be able to equally distract the anterior and posterior regions of the disc.

The finite element model developed in this work was "virtually" implanted with pedicle screws. Because many spinal devices are attached using pedicle screws, this model could be used to test many different types of posterior spinal devices. This could be advantageous in making comparisons between different spinal devices and highlighting potential advantages of one device over another.

Future versions of this model could include a displacement controlled model rather than a moment controlled model. A displacement controlled model would allow for further investigation into the effects of dynamic stabilization at the adjacent levels. Because the model used in this study employed a pure moment for exercising the spine segment, it is difficult to draw conclusions on the effects at the adjacent levels. When a pure moment is applied each

model could potentially have a different amount of displacement, making it difficult to make direct comparisons at the adjacent levels between each model. New versions of the model may also include improved material properties. The BABEL laboratory is currently working to characterize the material properties of spinal ligaments. It is anticipated that these improved material models will be implemented into future finite element models.

REFERENCES

[1] Katz, J. N., 2006, "Lumbar disc disorders and low-back pain: socioeconomic factors and consequences," The Journal of Bone and Joint Surgery, 88-A(Suppl 2), pp. 21-24.

[2] An, H. S., Anderson, P. A., Haughton, V. M., Iatridis, J. C., Kang, J. D., Lotz, J. C., Natarajan, R. N., Oegema, T. R., Jr., Roughley, P., Setton, L. A., Urban, J. P., Videman, T., Andersson, G. B., and Weinstein, J. N., 2004, "Introduction: disc degeneration: summary," Spine (Phila Pa 1976), 29(23), pp. 2677-2678.

[3] Cohen, S. P., Gallagher, R. M., Davis, S. A., Griffith, S. R., and Carragee, E. J., 2011, "Spine-area pain in military personnel: a review of epidemiology, etiology, diagnosis, and treatment," Spine J.

[4] Hilibrand, A. S., and Robbins, M., 2004, "Adjacent segment degeneration and adjacent segment disease: the consequences of spinal fusion?," The Spine Journal, 4(6), pp. S190-S194.

[5] Chou, W. Y., Hsu, C. J., Chang, W. N., and Wong, C. Y., 2002, "Adjacent segment degeneration after lumbar spinal posterolateral fusion with instrumentation in elderly patients," Arch Orthop Trauma Surg, 122(1), pp. 39-43.

[6] Kumar, M. N., Baklanov, A., and Chopin, D., 2001, "Correlation between sagittal plane changes and adjacent segment degeneration following lumbar spine fusion," Eur Spine J, 10(4), pp. 314-319.

[7] Lee, M. J. L., Joshua, D. Bransford, Richard J., 2010, "Pedicle Screw-based Posterior Dynamic Stabilization in the Lumbar Spine," Journal Am Acad Orthop Surg, 18(10), pp. 581-588.

[8] Lee, C. K., 1988, "Accelerated degeneration of the segment adjacent to a lumbar fusion," Spine (Phila Pa 1976), 13(3), pp. 375-377.

[9] Weinhoffer, S. L., Guyer, R. D., Herbert, M., and Griffith, S. L., 1995, "Intradiscal pressure measurements above an instrumented fusion. A cadaveric study," Spine (Phila Pa 1976), 20(5), pp. 526-531.

[10] Stoll, T. M., Dubois, G., and Schwarzenbach, O., 2002, "The dynamic neutralization system for the spine: a multi-center study of a novel non-fusion system," Eur Spine J, 11 Suppl 2, pp. S170-178.

[11] Sengupta, D. K., 2004, "Dynamic stabilization devices in the treatment of low back pain," Orthop Clin North Am, 35(1), pp. 43-56.

[12] Rohlmann, A., Zander, T., Bergmann, G., and Boustani, H. N., 2011, "Optimal stiffness of a pedicle-screw-based motion preservation implant for the lumbar spine," Eur Spine J.

[13] Lee, M. J., Lindsey, J. D., and Bransford, R. J., 2010, "Pedicle screw-based posterior dynamic stabilization in the lumbar spine," The Journal of the American Academy of Orthopaedic Surgeons, 18(10), pp. 581-588.

[14] Marchand, F., and Ahmed, A. M., 1990, "Investigation of the laminate structure of lumbar disc anulus fibrosus," Spine (Phila Pa 1976), 15(5), pp. 402-410.

[15] Inoue, N., and Orias, A. A., 2011, "Biomechanics of intervertebral disk degeneration," Orthop Clin North Am, 42(4), pp. 487-499, vii.

[16] Rohlmann, A., Zander, T., Schmidt, H., Wilke, H. J., and Bergmann, G., 2006, "Analysis of the influence of disc degeneration on the mechanical behaviour of a lumbar motion segment using the finite element method," J Biomech, 39(13), pp. 2484-2490.

[17] Schollum, M. L., Robertson, P. A., and Broom, N. D., 2008, "ISSLS prize winner: microstructure and mechanical disruption of the lumbar disc annulus: part I: a microscopic investigation of the translamellar bridging network," Spine (Phila Pa 1976), 33(25), pp. 2702-2710.

[18] Guerin, H. A., and Elliott, D. M., 2006, "Degeneration affects the fiber reorientation of human annulus fibrosus under tensile load," J Biomech, 39(8), pp. 1410-1418.

[19] O'Connell, G. D., Guerin, H. L., and Elliott, D. M., 2009, "Theoretical and uniaxial experimental evaluation of human annulus fibrosus degeneration," Journal of biomechanical engineering, 131(11), p. 111007.

[20] Veres, S. P., Robertson, P. A., and Broom, N. D., 2008, "ISSLS prize winner: microstructure and mechanical disruption of the lumbar disc annulus: part II: how the annulus fails under hydrostatic pressure," Spine (Phila Pa 1976), 33(25), pp. 2711-2720.

[21] Gillet, P., 2003, "The fate of the adjacent motion segments after lumbar fusion," J Spinal Disord Tech, 16(4), pp. 338-345.

[22] Lee, C. K., and Langrana, N. A., 1984, "Lumbosacral spinal fusion. A biomechanical study," Spine (Phila Pa 1976), 9(6), pp. 574-581.

[23] Kim, C. H., Chung, C. K., and Jahng, T. A., 2011, "Comparisons of outcomes after single or multilevel dynamic stabilization: effects on adjacent segment," J Spinal Disord Tech, 24(1), pp. 60-67.

[24] Niosi, C. A., Zhu, Q. A., Wilson, D. C., Keynan, O., Wilson, D. R., and Oxland, T. R., 2006, "Biomechanical characterization of the three-dimensional kinematic behaviour of the Dynesys dynamic stabilization system: an in vitro study," European spine journal : official publication of the European Spine Society, the European Spinal Deformity Society, and the European Section of the Cervical Spine Research Society, 15(6), pp. 913-922.

[25] Rohlmann, A., Burra, N. K., Zander, T., and Bergmann, G., 2007, "Comparison of the effects of bilateral posterior dynamic and rigid fixation devices on the loads in the lumbar spine: a finite element analysis," Eur Spine J, 16(8), pp. 1223-1231.

[26] Bono, C. M., Kadaba, M., and Vaccaro, A. R., 2009, "Posterior pedicle fixation-based dynamic stabilization devices for the treatment of degenerative diseases of the lumbar spine," J Spinal Disord Tech, 22(5), pp. 376-383.

[27] Hadlow, S. V., Fagan, A. B., Hillier, T. M., and Fraser, R. D., 1998, "The Graf ligamentoplasty procedure. Comparison with posterolateral fusion in the management of low back pain," Spine (Phila Pa 1976), 23(10), pp. 1172-1179.

[28] Mulholland, R. C., and Sengupta, D. K., 2002, "Rationale, principles and experimental evaluation of the concept of soft stabilization," Eur Spine J, 11 Suppl 2, pp. S198-205.

[29] Grevitt, M. P., Gardner, A. D., Spilsbury, J., Shackleford, I. M., Baskerville, R., Pursell, L. M., Hassaan, A., and Mulholland, R. C., 1995, "The Graf stabilisation system: early results in 50 patients," European spine journal : official publication of the European Spine Society, the European Spinal Deformity Society, and the European Section of the Cervical Spine Research Society, 4(3), pp. 169-175; discussion 135.

[30] Mulholland, R. C., and Sengupta, D. K., 2002, "Rationale, principles and experimental evaluation of the concept of soft stabilization," Eur Spine J, 11 Suppl 2, pp. S198-205.

[31] Stoll, T. M., Dubois, G., and Schwarzenbach, O., 2002, "The dynamic neutralization system for the spine: a multi-center study of a novel non-fusion system," Eur Spine J, 11 Suppl 2, pp. S170-178.

[32] Schilling, C., Kruger, S., Grupp, T. M., Duda, G. N., Blomer, W., and Rohlmann, A., 2011, "The effect of design parameters of dynamic pedicle screw systems on kinematics and load bearing: an in vitro study," European spine journal : official publication of the European Spine Society, the European Spinal Deformity Society, and the European Section of the Cervical Spine Research Society, 20(2), pp. 297-307.

[33] Schmoelz, W., Huber, J. F., Nydegger, T., Dipl, I., Claes, L., and Wilke, H. J., 2003, "Dynamic stabilization of the lumbar spine and its effects on adjacent segments: an in vitro experiment," J Spinal Disord Tech, 16(4), pp. 418-423.

[34] Schmoelz, W., Huber, J. F., Nydegger, T., Claes, L., and Wilke, H. J., 2006, "Influence of a dynamic stabilisation system on load bearing of a bridged disc: an in vitro study of intradiscal pressure," European spine journal : official publication of the European Spine Society, the European Spinal Deformity Society, and the European Section of the Cervical Spine Research Society, 15(8), pp. 1276-1285.

[35] Kumar, A., Beastall, J., Hughes, J., Karadimas, E. J., Nicol, M., Smith, F., and Wardlaw, D., 2008, "Disc changes in the bridged and adjacent segments after Dynesys dynamic stabilization system after two years," Spine (Phila Pa 1976), 33(26), pp. 2909-2914.

[36] Gornet, M. F., Chan, F. W., Coleman, J. C., Murrell, B., Nockels, R. P., Taylor, B. A., Lanman, T. H., and Ochoa, J. A., 2011, "Biomechanical assessment of a PEEK rod system for semi-rigid fixation of lumbar fusion constructs," J Biomech Eng, 133(8), p. 081009.

[37] Yue, J. J., Timm, J. P., Panjabi, M. M., and Jaramillo-de la Torre, J., 2007, "Clinical application of the Panjabi neutral zone hypothesis: the Stabilimax NZ posterior lumbar dynamic stabilization system," Neurosurg Focus, 22(1), p. E12.

[38] Dodgen, E., Stratton, E., Bowden, A.E., Howell, L.L., 2012, "Spinal Implant Development, Modeling, and Testing to Achieve Customizable and Nonlinear Stiffness," Journal of Medical Devices, 3(2).

[39] Howell, L. L., 2001, Compliant Mechanisms, John Wiley & Sons, Inc., New York.

[40] Zander, T., Krishnakanth, P., Bergmann, G., and Rohlmann, A., 2010, "Diurnal variations in intervertebral disc height affect spine flexibility, intradiscal pressure and contact compressive forces in the facet joints," Comput Methods Biomech Biomed Engin, 13(5), pp. 551-557.

[41] Zander, T., Bergmann, G., and Rohlmann, A., 2009, "Large sizes of vertebral body replacement do not reduce the contact pressure on adjacent vertebral bodies per se," Med Eng Phys, 31(10), pp. 1307-1312.

[42] Dreischarf, M., Rohlmann, A., Bergmann, G., and Zander, T., 2011, "Optimised loads for the simulation of axial rotation in the lumbar spine," J Biomech, 44(12), pp. 2323-2327.

[43] Dreischarf, M., Zander, T., Bergmann, G., and Rohlmann, A., 2010, "A non-optimized follower load path may cause considerable intervertebral rotations," J Biomech, 43(13), pp. 2625-2628.

[44] Shirazi-Adl, A., 1994, "Nonlinear stress analysis of the whole lumbar spine in torsion--mechanics of facet articulation," J Biomech, 27(3), pp. 289-299.

[45] Shirazi-Adl, A., 1994, "Biomechanics of the lumbar spine in sagittal/lateral moments," Spine (Phila Pa 1976), 19(21), pp. 2407-2414.

[46] Shirazi-Adl, A., and Parnianpour, M., 2000, "Load-bearing and stress analysis of the human spine under a novel wrapping compression loading," Clin Biomech (Bristol, Avon), 15(10), pp. 718-725.

[47] Shirazi-Adl, A., Sadouk, S., Parnianpour, M., Pop, D., and El-Rich, M., 2002, "Muscle force evaluation and the role of posture in human lumbar spine under compression," Eur Spine J, 11(6), pp. 519-526.

[48] Bhattacharya, S., Goel, V. K., Liu, X., Kiapour, A., and Serhan, H. A., 2011, "Models that incorporate spinal structures predict better wear performance of cervical artificial discs," Spine J, 11(8), pp. 766-776.

[49] Goel, V. K., and Clausen, J. D., 1998, "Prediction of load sharing among spinal components of a C5-C6 motion segment using the finite element approach," Spine (Phila Pa 1976), 23(6), pp. 684-691.

[50] Goel, V. K., Faizan, A., Palepu, V., and Bhattacharya, S., 2011, "Parameters that effect spine biomechanics following cervical disc replacement," Eur Spine J.

[51] Goel, V. K., Monroe, B. T., Gilbertson, L. G., and Brinckmann, P., 1995, "Interlaminar shear stresses and laminae separation in a disc. Finite element analysis of the L3-L4 motion segment subjected to axial compressive loads," Spine (Phila Pa 1976), 20(6), pp. 689-698.

[52] Ahn, Y. H., Chen, W. M., Lee, K. Y., Park, K. W., and Lee, S. J., 2008, "Comparison of the load-sharing characteristics between pedicle-based dynamic and rigid rod devices," Biomed Mater, 3(4), p. 044101.

[53] Schmidt, H., Heuer, F., Claes, L., and Wilke, H. J., 2008, "The relation between the instantaneous center of rotation and facet joint forces - A finite element analysis," Clinical biomechanics, 23(3), pp. 270-278.

[54] Schmidt, H., Heuer, F., and Wilke, H. J., 2009, "Which axial and bending stiffnesses of posterior implants are required to design a flexible lumbar stabilization system?," J Biomech, 42(1), pp. 48-54.

[55] Schmidt, H., Kettler, A., Rohlmann, A., Claes, L., and Wilke, H. J., 2007, "The risk of disc prolapses with complex loading in different degrees of disc degeneration - a finite element analysis," Clin Biomech (Bristol, Avon), 22(9), pp. 988-998.

[56] Bowden, A. E., Guerin, H. L., Villarraga, M. L., Patwardhan, A. G., and Ochoa, J. A., 2008, "Quality of motion considerations in numerical analysis of motion restoring implants of the spine," Clin Biomech (Bristol, Avon), 23(5), pp. 536-544.

[57] Rundell, S. A., Auerbach, J. D., Balderston, R. A., and Kurtz, S. M., 2008, "Total disc replacement positioning affects facet contact forces and vertebral body strains," Spine (Phila Pa 1976), 33(23), pp. 2510-2517.

[58] Rundell, S. A., Guerin, H. L., Auerbach, J. D., and Kurtz, S. M., 2009, "Effect of nucleus replacement device properties on lumbar spine mechanics," Spine (Phila Pa 1976), 34(19), pp. 2022-2032.

[59] Wilke, H. J., Rohlmann, F., Neidlinger-Wilke, C., Werner, K., Claes, L., and Kettler, A., 2006, "Validity and interobserver agreement of a new radiographic grading system for intervertebral disc degeneration: Part I. Lumbar spine," European spine journal : official publication of the European Spine Society, the European Spinal Deformity Society, and the European Section of the Cervical Spine Research Society, 15(6), pp. 720-730.

[60] Rohlmann, A., Nabil Boustani, H., Bergmann, G., and Zander, T., 2010, "Effect of a pedicle-screw-based motion preservation system on lumbar spine biomechanics: A probabilistic

finite element study with subsequent sensitivity analysis," Journal of Biomechanics, 43(15), pp. 2963-2969.

[61] Schmidt, H., Heuer, F., Drumm, J., Klezl, Z., Claes, L., and Wilke, H. J., 2007, "Application of a calibration method provides more realistic results for a finite element model of a lumbar spinal segment," Clin Biomech (Bristol, Avon), 22(4), pp. 377-384.

[62] Ulrich, D., van Rietbergen, B., Laib, A., and Ruegsegger, P., 1999, "The ability of three-dimensional structural indices to reflect mechanical aspects of trabecular bone," Bone, 25(1), pp. 55-60.

[63] Morgan, E. F., Bayraktar, H. H., and Keaveny, T. M., 2003, "Trabecular bone modulus-density relationships depend on anatomic site," J Biomech, 36(7), pp. 897-904.

[64] Polikeit, A., Nolte, L. P., and Ferguson, S. J., 2003, "The effect of cement augmentation on the load transfer in an osteoporotic functional spinal unit: finite-element analysis," Spine (Phila Pa 1976), 28(10), pp. 991-996.

[65] Elliott, D. M., and Setton, L. A., 2001, "Anisotropic and inhomogeneous tensile behavior of the human anulus fibrosus: experimental measurement and material model predictions," J Biomech Eng, 123(3), pp. 256-263.

[66] Galbusera, F., Bellini, C. M., Anasetti, F., Ciavarro, C., Lovi, A., and Brayda-Bruno, M., 2011, "Rigid and flexible spinal stabilization devices: a biomechanical comparison," Med Eng Phys, 33(4), pp. 490-496.

[67] Wilke, H. J., Heuer, F., and Schmidt, H., 2009, "Prospective design delineation and subsequent in vitro evaluation of a new posterior dynamic stabilization system," Spine (Phila Pa 1976), 34(3), pp. 255-261.

[68] Chazal, J., Tanguy, A., Bourges, M., Gaurel, G., Escande, G., Guillot, M., and Vanneuville, G., 1985, "Biomechanical properties of spinal ligaments and a histological study of the supraspinal ligament in traction," Journal of Biomechanics, 18(3), pp. 167-176.

[69] Patwardhan, A. G., Havey, R. M., Meade, K. P., Lee, B., and Dunlap, B., 1999, "A follower load increases the load-carrying capacity of the lumbar spine in compression," Spine (Phila Pa 1976), 24(10), pp. 1003-1009.

[70] Kurtz, S. M., Edidin, A.A., 2006, Spine Technology Handbook, Elsevier Academic Press, Burlington, MA.

[71] Panjabi, M. M., Oxland, T. R., Yamamoto, I., and Crisco, J. J., 1994, "Mechanical behavior of the human lumbar and lumbosacral spine as shown by three-dimensional load-displacement curves," J Bone Joint Surg Am, 76(3), pp. 413-424.

[72] Fujiwara, A., Lim, T. H., An, H. S., Tanaka, N., Jeon, C. H., Andersson, G. B., and Haughton, V. M., 2000, "The effect of disc degeneration and facet joint osteoarthritis on the segmental flexibility of the lumbar spine," Spine (Phila Pa 1976), 25(23), pp. 3036-3044.

[73] Schmoelz, W., Huber, J. F., Nydegger, T., Dipl, I., Claes, L., and Wilke, H. J., 2003, "Dynamic stabilization of the lumbar spine and its effects on adjacent segments: an in vitro experiment," J Spinal Disord Tech, 16(4), pp. 418-423.

[74] Frei, H., Oxland, T. R., Rathonyi, G. C., and Nolte, L. P., 2001, "The effect of nucleotomy on lumbar spine mechanics in compression and shear loading," Spine (Phila Pa 1976), 26(19), pp. 2080-2089.

[75] Pearcy, M. J., and Bogduk, N., 1988, "Instantaneous axes of rotation of the lumbar intervertebral joints," Spine (Phila Pa 1976), 13(9), pp. 1033-1041.

[76] Benzel, 2011, "Mechanical Characterization of a Viscoelastic Disc for Lumbar Total Disc Replacement," Journal of Medical Devices.

[77] Sengupta, D. K., and Mulholland, R. C., 2005, "Fulcrum assisted soft stabilization system: a new concept in the surgical treatment of degenerative low back pain," Spine (Phila Pa 1976), 30(9), pp. 1019-1029; discussion 1030.

[78] Bryndza, J., Weiser, A., Paliwal, M., 2009, "Design of a Dynamic Stabilization Spine Implant," Journal of Medical Devices, 3(2).

[79] Zirbel, S. A., Stolworthy, D.K., Howell, L.L., and Bowden, A.E., 2012, "Intervertebral Disc Degeneration Alters Lumbar Spine Segmental Stiffness in All Modes of Loading Under a Compressive Follower Load," The Spine Journal.

[80] Natarajan, R. N., and Andersson, G. B., 1999, "The influence of lumbar disc height and cross-sectional area on the mechanical response of the disc to physiologic loading," Spine (Phila Pa 1976), 24(18), pp. 1873-1881.

[81] Fan, C.-Y., Hsu, C.-C., Chao, C.-K., Lin, S.-C., and Chao, K.-H., 2010, "Biomechanical comparisons of different posterior instrumentation constructs after two-level ALIF: A finite element study," Medical Engineering & Physics, 32(2), pp. 203-211.

[82] Meakin, J. R., 2001, "Replacing the nucleus pulposus of the intervertebral disk: prediction of suitable properties of a replacement material using finite element analysis," J Mater Sci Mater Med, 12(3), pp. 207-213.

[83] LSTC, 2007, "LS-DYNA KEYWORD USER'S MANUAL," 1.

[84] Weinans, H., Sumner, D. R., Igloria, R., and Natarajan, R. N., 2000, "Sensitivity of periprosthetic stress-shielding to load and the bone density-modulus relationship in subject-specific finite element models," J Biomech, 33(7), pp. 809-817.

[85] Kerner, J., Huiskes, R., van Lenthe, G. H., Weinans, H., van Rietbergen, B., Engh, C. A., and Amis, A. A., 1999, "Correlation between pre-operative periprosthetic bone density and post-operative bone loss in THA can be explained by strain-adaptive remodelling," J Biomech, 32(7), pp. 695-703.

[86] Cho, B. Y., Murovic, J., Park, K. W., and Park, J., 2010, "Lumbar disc rehydration postimplantation of a posterior dynamic stabilization system," J Neurosurg Spine, 13(5), pp. 576-580.

[87] Schnake, K. J., Putzier, M., Haas, N. P., and Kandziora, F., 2006, "Mechanical concepts for disc regeneration," Eur Spine J, 15 Suppl 3, pp. S354-360.

[88] Meyers, K., Tauber, M., Sudin, Y., Fleischer, S., Arnin, U., Girardi, F., and Wright, T., 2008, "Use of instrumented pedicle screws to evaluate load sharing in posterior dynamic stabilization systems," The Spine Journal, 8(6), pp. 926-932.

APPENDIX A.   LS-DYNA INPUT DECKS

This appendix includes the input decks used in LS-DYNA.

A.1   Loading Files

A.1.1   Applying Follower Load

```
*KEYWORD
*TITLE
JEFFS_MODEL
*INCLUDE
fluidmaterials.k
*INCLUDE
mesh312.k
*INCLUDE
temps_jeff.k
*BOUNDARY_SPC_SET
1,,1,1,1
*BOUNDARY_SPC_SET
1000,,1,1,1
*CONSTRAINED_EXTRA_NODES_SET
1,100
*CONSTRAINED_RIGID_BODIES
1,67
1,68
*CONSTRAINED_NODAL_RIGID_BODY_TITLE
LeftSup
1,,200
*CONSTRAINED_NODAL_RIGID_BODY_TITLE
LeftInf
2,,201
*CONSTRAINED_NODAL_RIGID_BODY_TITLE
RightSup
3,,300
*CONSTRAINED_NODAL_RIGID_BODY_TITLE
RightInf
4,,301
*CONTROL_CONTACT
```

```
,,2


,,,,1

*CONTROL_ENERGY
2
*CONTROL_PARALLEL
12,0,0,0
*CONTROL_SHELL
,1,,,2,2,1
,1

*CONTROL_TERMINATION
30
*CONTROL_TIMESTEP
,0.8,,,-6e-010

*DAMPING_GLOBAL
,2
*DATABASE_BNDOUT
1,,,1
*DATABASE_GLSTAT
1,,,1
*DATABASE_MATSUM
1,,,1
*DATABASE_RBDOUT
1,,,1
*DATABASE_RCFORC
0.002,,,1
*DATABASE_BINARY_D3PLOT
10

*DATABASE_EXTENT_BINARY
,,,1

,,1,,,,STRESS,STRESS
*CONTACT_SURFACE_TO_SURFACE_ID
1,L1Inferior-L2Superior
1,3
,,,,,,,1e+020
1,1,,,1,1,1,1
*CONTACT_SURFACE_TO_SURFACE_ID
2,L2Inferior-L3Superior
2,4
,,,,,,,1e+020
1,1,,,1,1,1,1
*CONTACT_SURFACE_TO_SURFACE_ID
3,L3Inferior-L4Superior
5,6
,,,,,,,1e+020
1,1,,,1,1,1,1
*CONTACT_SURFACE_TO_SURFACE_ID
4,L4Inferior-L5Superior
7,8
,,,,,,,1e+020
```

```
1,1,,,1,1,1,1
*CONTACT_SURFACE_TO_SURFACE_ID
5,L5-Sacrum
9,10
,,,,,,,1e+020
1,1,,,1,1,1,1
*CONTACT_NODES_TO_SURFACE_ID
6,T12-L1Superior
111,11,4

0.05,1,,,1,1,1,1
*CONTACT_SURFACE_TO_SURFACE_ID
7,LeftSuperiorSpar
12,14
,,,,,,,1e+020
1,1,,,1,1,1,1

*CONTACT_SURFACE_TO_SURFACE_ID
8,LeftInferiorSpar
13,15
,,,,,,,1e+020
1,1,,,1,1,1,1
*CONTACT_SURFACE_TO_SURFACE_ID
9,RightSuperiorSpar
16,18
,,,,,,,1e+020
1,1,,,1,1,1,1
*CONTACT_SURFACE_TO_SURFACE_ID
10,RightInferiorSpar
17,19
,,,,,,,1e+020
1,1,,,1,1,1,1
*CONTACT_SINGLE_SURFACE_ID
11,LeftTop
20
,,,,,,,1e+020
1,1,,,1,1,1,1
*CONTACT_SINGLE_SURFACE_ID
12,LeftBottom
21
,,,,,,,1e+020
1,1,,,1,1,1,1
*CONTACT_SINGLE_SURFACE_ID
13,RightTop
22
,,,,,,,1e+020
1,1,,,1,1,1,1
*CONTACT_SINGLE_SURFACE_ID
14,RightBottom
23
,,,,,,,1e+020
1,1,,,1,1,1,1

*LOAD_RIGID_BODY
1,5,1,1
*DEFINE_CURVE
1
```

```
0,0
30,0
320,0
$$$$$$$$$$$$$$$$$$$$$$$$$$$   LATERAL  $$$$$$$$$$$$$$$$$$$$$$$$$$$
*LOAD_RIGID_BODY
1,6,2,1
*DEFINE_CURVE
2
0,0
30,0
320,0
$$$$$$$$$$$$$$$$$$$$$$$$$$$   AXIAL  $$$$$$$$$$$$$$$$$$$$$$$$$$$
*LOAD_RIGID_BODY
1,7,3,1
*DEFINE_CURVE
3
0,0
30,0
320,0
*END
```

A.1.2   Restart Deck After Follower Load Complete

```
*KEYWORD
*CONTROL_TERMINATION
320
*DAMPING_GLOBAL
0,.19
*DATABASE_BINARY_D3PLOT
1
*CHANGE_CURVE_DEFINITION
1
*DEFINE_CURVE
1
0,0
30,0
320,6000
*END
```

A.2   Materials

A.2.1   T12 Interface (Rigid Body)

```
*MAT_RIGID
1,1.9130E-03,999.7398,0.200,,,
0,0,0
0
*DEFINE_COORDINATE_SYSTEM
1,0.004,-16.536,0.065,1.00339,-16.536,0.1
0.004,-15.5366,0.1
*HOURGLASS
```

```
1,1,0.0,0,0.0,0.0
*SECTION_SHELL
1,1,0.0,3.0,0.0,0.0,0
0.25,0.25,0.25,0.25,0.0
*PART
T12 Interface
1,1,1,0,1,0,0,0
```

A.2.2 Vertebrae

```
*MAT_TEMPERATURE_DEPENDENT_ORTHOTROPIC
2,1.8745E-03,2
,,,1,0,0
,,,1,1,0
4.2,2.9,10.0,0.23,0.40,0.38
0.00,0.00,0.00,1.53,1.83,1.31,-1000
4.2,2.9,10.0,0.23,0.40,0.38
0.00,0.00,0.00,1.53,1.83,1.31,74.999
0.647,0.446,1.539,0.23,0.40,0.38
0.00,0.00,0.00,0.236,0.281,0.201,75
8.089,5.585,19.259,0.23,0.40,0.38
0.00,0.00,0.00,2.950,3.521,2.518,125
23.927,16.521,56.969,0.23,0.40,0.38
0.00,0.00,0.00,8.728,10.415,7.449,188
28.368,19.588,67.543,0.23,0.40,0.38
0.00,0.00,0.00,10.348,12.349,8.832,200
48.559,33.529,115.617,0.23,0.40,0.38
0.00,0.00,0.00,17.713,21.138,15.118,250
72.371,49.970,172.312,0.23,0.40,0.38
0.00,0.00,0.00,26.398,31.503,22.531,300
110.770,76.484,263.738,0.23,0.40,0.38
0.00,0.00,0.00,40.405,48.218,34.486,370
159.975,110.459,380.893,0.23,0.40,0.38
0.00,0.00,0.00,58.353,69.637,49.806,400
253.604,175.107,603.818,0.23,0.40,0.38
0.00,0.00,0.00,92.506,110.393,78.955,450
361.772,249.795,861.362,0.23,0.40,0.38
0.00,0.00,0.00,131.962,157.478,112.632,500
432.071,298.335,1028.741,0.23,0.40,0.38
0.00,0.00,0.00,157.605,188.079,134.518,530
1256.983,867.917,2992.818,0.23,0.40,0.38
0.00,0.00,0.00,458.505,547.161,391.341,800
2046.174,1412.835,4871.843,0.23,0.40,0.38
0.00,0.00,0.00,746.375,890.693,637.042,1000
4556.743,3146.322,10849.387,0.23,0.40,0.38
0.00,0.00,0.00,1662.144,1983.535,1418.666,1500
7714.551,5326.714,18367.979,0.23,0.40,0.38
0.00,0.00,0.00,2814.005,3358.120,2401.797,2000
15637.338,10797.210,37231.758,0.23,0.40,0.38
0.00,0.00,0.00,5703.968,6806.883,4868.426,3000
25385.609,17528.158,60441.925,0.23,0.40,0.38
0.00,0.00,0.00,9259.804,11050.274,7903.388,4000
36720.751,25354.804,87430.358,0.23,0.40,0.38
0.00,0.00,0.00,13394.477,15984.425,11432.396,5000
```

```
*HOURGLASS
2,1,0.0,0,0.0,0.0
*SECTION_SOLID
2,1,0,0
*PART
L1 Vertebra
2,2,2,0,2,0,0,0

*MAT_ELASTIC
69,1.914E-03,12000.0,0.2,,,
*HOURGLASS
69,1,0.0,0,0.0,0.0
*SECTION_SHELL
69,1,0.0,3.0,0.0,0.0,0
0.4,0.4,0.4,0.4,0.0
*PART
Cortical Bone
69,69,69,0,69,0,0,0
```

A.2.3   Intervertebral Discs

```
*MAT_ELASTIC_FLUID
8,1.0003E-03,1,.49,,,1720
.3,1.0e20
*HOURGLASS
8,6,1.0,0,0.0,0.0
*SECTION_SOLID
8,1,0
*PART
Nucleus Pulposus T12-L1
8,8,8,0,8,0,0,0
*MAT_ORTHOTROPIC_ELASTIC
9,1.0003E-03,5.5999,0.3400,0.1900,0.107,0.0112,0.0782
0.1000,0.1000,0.1000,4.0,6.894E-007
8.715,97.176,234.350
0.1265,-0.3813,0.7990
*HOURGLASS
9,6,1.0,0,0.0,0.0
*SECTION_SOLID
9,1,0
*PART
Inner AF T12-L1
9,9,9,0,9,0,0,0
*MAT_ORTHOTROPIC_ELASTIC
10,1.0003E-03,20.9,.42,.29,0.0456,0.0110,0.4212
0.1000,0.1000,0.1000,4.0,6.894E-007
8.715,97.176,234.350
0.1265,-0.3813,0.7990
*HOURGLASS
10,6,1.0,0,0.0,0.0
*SECTION_SOLID
10,1,0
*PART
```

```
Outer AF T12-L1
10,10,10,0,10,0,0,0
```

A.2.3   Ligaments

```
*MAT_FABRIC
26,1.0003E-03,2,2,2,0.3,0.3,0.3
0.0,0.0,0.0,1.0,0.0,0.0,0.0,0.5
0.0,0.0,0.0,0.0,0.0,4
0.0,0.0,0.0,0.0,0.0,0.0
0.0,0.0,0.0,0.0,0.0,0.0
26
*HOURGLASS
26,0,0.0,0,0.0,0.0
*SECTION_SHELL
26,1,0.0,3.0,0.0,0.0,1
0.9398,0.9398,0.9398,0.9398,0.0
0,90,0
*PART
ALL
26,26,26,0,26,0,0,0
*DEFINE_CURVE
26,0,0.0,0.0,0.0,0.0,0
0.0,0.0
0.12,1.15
0.44,9.11
0.57,10.3
```

A.2.4   Pedicle Screws

```
*MAT_ELASTIC
32,0.00443,113800,0.342
*HOURGLASS
32,1,0.0,0,0.0,0.0
*SECTION_SOLID
32,1,0,0
*PART
Pedicle Screws
32,32,32,0,32,0,0,0
```

A.2.5   Follower Load

```
*MAT_ELASTIC_SPRING_DISCRETE_BEAM
35,0.002,.001,444

*HOURGLASS
35,1,0.0,0,0.0,0.0
*SECTION_BEAM
35,6

*PART
FOLLOWER
```

```
35,35,35,0,35,0,0,0
```

A.2.6 FlexSPAR

```
*MAT_ELASTIC
74,0.443,113800,0.342
*HOURGLASS
74,1,0.0,0,0.0,0.0
*SECTION_SOLID
74,1,0,0
*PART
FlexSpar
74,74,74,0,74,0,0,0
```

A.2.7 Inserts

```
*MAT_ELASTIC
75,0.132,3700,0.4
*HOURGLASS
75,1,0.0,0,0.0,0.0
*SECTION_SOLID
75,1,0,0
*PART
Insert
75,75,75,0,75,0,0,0
```

A.3 PBS Script

```
#!/bin/bash

#PBS -l nodes=1:ppn=12,mem=9gb,walltime=100:00:00
#PBS -N jobname
#PBS -m bea
#PBS -M harris.jeff@gmail.com

# Set the max number of threads to use for programs using OpenMP. Should be
<= ppn. Does nothing if the program doesn't use OpenMP.
export OMP_NUM_THREADS=12
export LSTC_LICENSE=network
export LSTC_LICENSE_SERVER=fsllinuxlic4
export LSTC_LICENSE_SERVER_PORT=13373

# The following line changes to the directory that you submit your job from
cd "$PBS_O_WORKDIR"

/fslhome/harrisj/fsl_groups/fslg_babel/lsdyna/ls971d i=loadingfile.k
memory=1000m ncpu=12

exit 0
```